Chemical composition of Asian continental outflow over the western Pacific: Results from Transport and Chemical Evolution over the Pacific (TRACE-P)

R. S. Russo,[1] R. W. Talbot,[1] J. E. Dibb,[1] E. Scheuer,[1] G. Seid,[1] C. E. Jordan,[3]
H. E. Fuelberg,[2] G. W. Sachse,[3] M. A. Avery,[3] S. A. Vay,[3] D. R. Blake,[4] N. J. Blake,[4]
E. Atlas,[5] A. Fried,[5] S. T. Sandholm,[6] D. Tan,[6] H. B. Singh,[7] J. Snow,[8] and B. G. Heikes[8]

[1] We characterize the chemical composition of Asian continental outflow observed during the NASA Transport and Chemical Evolution over the Pacific (TRACE-P) mission during February–April 2001 in the western Pacific using data collected on the NASA DC-8 aircraft. A significant anthropogenic impact was present in the free troposphere and as far east as 150°E longitude reflecting rapid uplift and transport of continental emissions. Five-day backward trajectories were utilized to identify five principal Asian source regions of outflow: central, coastal, north-northwest (NNW), southeast (SE), and west-southwest (WSW). The maximum mixing ratios for several species, such as CO, C_2Cl_4, CH_3Cl, and hydrocarbons, were more than a factor of 2 larger in the boundary layer of the central and coastal regions due to industrial activity in East Asia. CO was well correlated with C_2H_2, C_2H_6, C_2Cl_4, and CH_3Cl at low altitudes in these two regions ($r^2 \sim$ 0.77–0.97). The NNW, WSW, and SE regions were impacted by anthropogenic sources above the boundary layer presumably due to the longer transport distances of air masses to the western Pacific. Frontal and convective lifting of continental emissions was most likely responsible for the high altitude outflow in these three regions. Photochemical processing was influential in each source region resulting in enhanced mixing ratios of O_3, PAN, HNO_3, H_2O_2, and CH_3OOH. The air masses encountered in all five regions were composed of a complex mixture of photochemically aged air with more recent emissions mixed into the outflow as indicated by enhanced hydrocarbon ratios ($C_2H_2/CO \geq 3$ and $C_3H_8/C_2H_6 \geq 0.2$). Combustion, industrial activities, and the burning of biofuels and biomass all contributed to the chemical composition of air masses from each source region as demonstrated by the use of C_2H_2, C_2Cl_4, and CH_3Cl as atmospheric tracers. Mixing ratios of O_3, CO, C_2H_2, C_2H_6, SO_2, and C_2Cl_4 were compared for the TRACE-P and PEM-West B missions. In the more northern regions, O_3, CO, and SO_2 were higher at low altitudes during TRACE-P. In general, mixing ratios were fairly similar between the two missions in the southern regions. A comparison between CO/CO_2, CO/CH_4, C_2H_6/C_3H_8, NO_x/SO_2, and $NO_y/(SO_2 + nss\text{-}SO_4)$ ratios for the five source regions and for the 2000 Asian emissions summary showed very close agreement indicating that Asian emissions were well represented by the TRACE-P data and the emissions inventory.   *INDEX TERMS:* 0365 Atmospheric Composition and Structure: Troposphere—composition and chemistry; 0368 Atmospheric Composition and Structure: Troposphere—constituent transport and chemistry; 0345 Atmospheric Composition and Structure: Pollution—urban and regional (0305)

[1]University of New Hampshire, Durham, New Hampshire, USA.
[2]Florida State University, Tallahassee, Florida, USA.
[3]NASA Langley Research Center, Hampton, Virginia, USA.
[4]University of California, Irvine, Irvine, California, USA.
[5]National Center for Atmospheric Research, Boulder, Colorado, USA.
[6]Georgia Institute of Technology, Atlanta, Georgia, USA.
[7]NASA Ames Research Center, Moffett Field, California, USA.
[8]University of Rhode Island, Narragansett, Rhode Island, USA.

1. Introduction

[2] The impact of industrialization and population growth in Asia on the composition of the western Pacific troposphere over the last several decades was not well documented, but it is likely to have been very significant. Recently, Asian anthropogenic emissions have been increasing, and for some species, such as SO_2 and NO_x, they are projected to continue increasing over the next 20 years [*Streets and Waldhoff*, 2000; *van Aardenne et al.*, 1999]. By

2020, China is predicted to be the largest emitter of NO_x in the world [*van Aardenne et al.*, 1999]. However, *Streets et al.* [2003] revealed that the economic downturn in Asia in the late 1990s resulted in lower SO_2 and NO_x emissions than expected. Owing to the potential of Asian emissions to modify the global tropospheric composition, it is crucial to the global community and to the formation of environmental policies to characterize and document these temporal variations in Asian emissions.

[3] It is well documented that Asian anthropogenic emissions and dust are transported over the North Pacific Ocean [e.g., *Duce et al.*, 1980; *Merrill et al.*, 1989; *Jaffe et al.*, 1999]. Several studies have documented the influence of Asian outflow on the western U. S. and the impact of rising Asian emissions on the global troposphere [e.g., *Berntsen et al.*, 1999; *Jacob et al.*, 1999; *Yienger et al.*, 2000]. The magnitude of this impact varies throughout the year due to different meteorological situations in the various seasons. During the summer and fall, the Pacific high is located over the western Pacific and inhibits outflow from the Asian continent. The high causes an easterly flow of aged marine air to the western Pacific. In the spring, this high-pressure system is displaced eastward allowing the rapid and direct transport of continental outflow from Asia to the western Pacific [*Bachmeier et al.*, 1996]. A strong Siberian high-pressure system is also present during winter [*Fuelberg et al.*, 2003]. These two high-pressure systems result in maximum outflow from the Asian continent occurring in the late winter and spring [*Merrill et al.*, 1989, 1997].

[4] Two previous aircraft missions were conducted to document the impact of seasonal variations in Asian outflow on the western Pacific. The Pacific Exploratory Mission (PEM)-West A was conducted in September–October 1991, and PEM-West B occurred in February–March 1994. Asian outflow was found to be the main contributor to the tropospheric composition below 5 km [*Talbot et al.*, 1997; *Gregory et al.*, 1997]. PEM-West B was characterized by two-fold enhancements in anthropogenic species, such as C_2H_2, C_2H_6, and C_3H_8, and decreased photochemical activity compared to PEM-West A. Increased source emissions and the winter/spring time period of PEM-West B were the presumed explanations for these differences. Wet convection was an important mechanism for transporting air to the upper troposphere during both missions [*Talbot et al.*, 1997]. The PEM-West missions provided valuable documentation of the trace gas and aerosol signatures of Asian outflow and information about the impact of Asian emissions on the western Pacific troposphere.

[5] A wide variety of pollution sources contribute emissions to the western Pacific troposphere because of differences in demographic and industrialization patterns. This results in specific sources being more predominant in certain regions of Asia. Fossil fuel combustion (e.g., electrical power generation) is the primary source of energy in Asia leading to emissions of SO_2, CO, CO_2, hydrocarbons, and reactive nitrogen species. China is the largest Asian source of SO_2 because of its use of high sulfur coal as a primary energy source [*Streets et al.*, 2003; *Carmichael et al.*, 2003b; *Kato and Akimoto*, 1992]. Biofuels (e.g., crop residues, fuel wood, animal waste, and charcoal) are estimated to be ~24 % of the total energy use [*Streets and Waldhoff*, 1998]. Biofuels are typically used for cooking and

heating and are the dominant energy source in developing countries. Also, biomass burning is widespread in southeast Asia [*Crutzen and Andreae*, 1990]. As a result, emissions of CO, hydrocarbons, CH_3Cl, and nitrogen species are expected from SE Asia. The domestic sector of central China is an important source of both fossil fuel and biofuel emissions [*Carmichael et al.*, 2003b]. Industrial activities (i.e., petroleum refining, solvent usage, fuel evaporation during storage and transport, and natural gas leakage) have a considerable impact on the tropospheric composition of East Asia and result in emissions of C_2Cl_4, CCl_4, CH_3CCl_3, and CFCs [*Blake et al.*, 1996]. Also, biogenic (i.e., vegetation, ocean) emission and uptake processes influence the composition of the western Pacific [e.g., *Talbot et al.*, 1996a, 1997].

[6] The focus of the NASA TRACE-P mission was to provide a comprehensive assessment of the impact of these various pollution sources on the atmospheric composition of the western Pacific and to study the chemical evolution and aging of Asian outflow. A secondary goal of TRACE-P was to determine if increasing Asian emissions over the past decade had a measurable impact on the tropospheric chemistry over the western Pacific and if the emission projections were substantially correct. A variety of methods were used to analyze and study the TRACE-P data, including examining the partitioning of specific species, models, emission inventories, meteorology patterns, transport mechanisms, and air mass trajectories. The results are presented in the many companion papers in this issue. In this paper we characterize and compare the chemical composition of outflow originating from the predominant source regions identified on the Asian continent and its transport to the western Pacific.

2. Experiment

[7] The TRACE-P mission was conducted during February–April 2001. The scientific rationale for the mission, species measurement details, and descriptions of the individual flights are presented in the TRACE-P overview paper [*Jacob et al.*, 2003]. The large-scale meteorology of the region during February–April 2001 and air mass trajectory details are described by *Fuelberg et al.* [2003]. The measurements used in this paper were made on the NASA Dryden DC-8 aircraft. The mission was composed of 17 transit and science intensive flights in the geographic region of 0–50°N latitude and 110–180°E longitude. The aircraft flew at altitudes ranging from 0.3 to 12.5 km. Flight 6 was a transit flight from Guam to Hong Kong, Flights 7–12 were based out of Hong Kong, and Flights 13–17 were based out of Yokota Air Force Base, Japan.

3. Database

[8] The data utilized in this paper was collected during Flights 6–17 within the geographic region of 10–45°N latitude and 110–150°E longitude. Merged data products for specific time intervals were created by NASA Langley Research Center due to the wide range of measurement time resolutions for the various species. The data presented in this paper was averaged to a 1 min time resolution. Measurements reported as below the limit of detection of
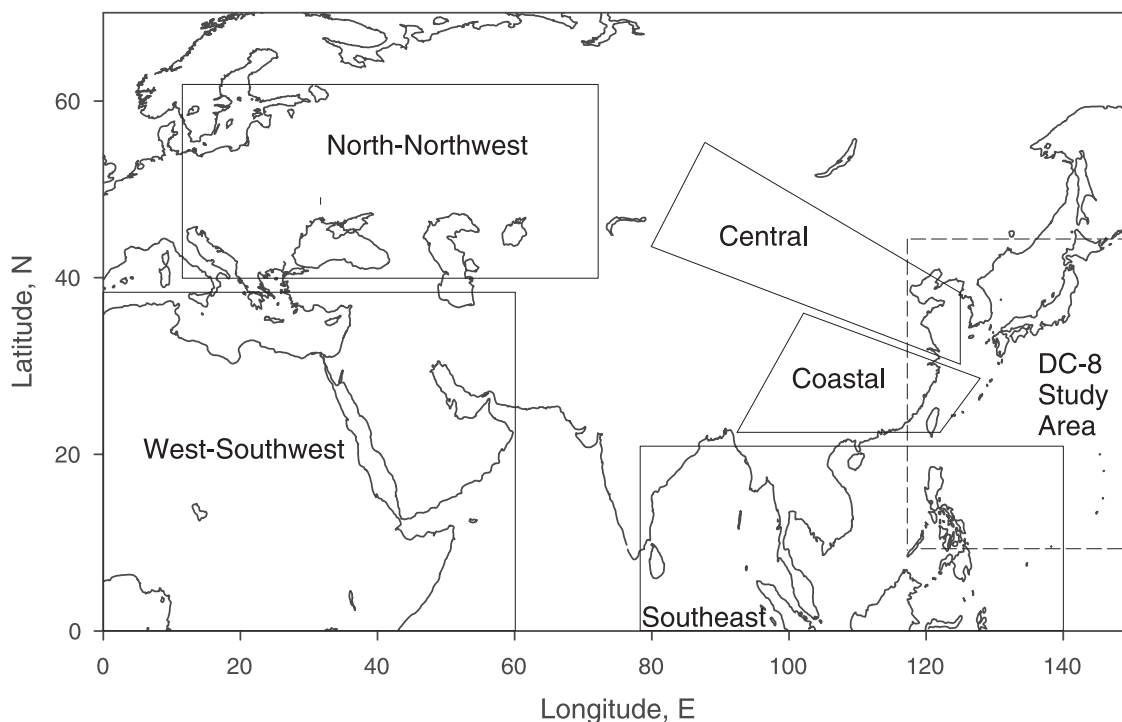
Figure 1. General locations of the five source regions of Asian continental outflow determined from 5-day backward trajectories. Data was collected within the geographic region 10–45°N and 110–150°E indicated by the dashed line box. This region only represents the DC-8 study area for Flights 6–17.

the instrument or that were influenced by stratospheric air were not included in the analysis. Stratospherically influenced air was defined as O_3 above 100 ppbv and CO less than ~70 ppbv (Northern Hemispheric background mixing ratio). When enhancements of both species were observed, the data was not removed from the database and was considered to be a mix of stratospheric and polluted air.

[9] Five-day backward trajectories, calculated by Florida State University [*Fuelberg et al.*, 2003], were used to identify continental source regions of outflow. Only measurements made during constant altitude flight legs were separated into the source region designations while data collected during the spiral ascents and descents was not included due to spatial heterogeneity in the air masses. Transport was dominated by strong westerly flow off of the Asian continent. Trajectories that did not travel over a continent, which was an infrequent occurrence, were not included in any of the source region groups.

[10] Examination of the five-day backward trajectories indicated that there were five general source regions of outflow (Figure 1). The five regions and their approximate latitude and longitude ranges are: central (30–60°N, 80–130°E), coastal (20–40°N, 90–130°E), southeast (SE) (0–25°N, 80–140°E), north-northwest (NNW) (40–65°N, 10–70°E), and west-southwest (WSW) (0–40°N, 0–60°E). These five source regions represent the general positions of the air masses five days prior to when they were encountered by the DC-8 over the western Pacific. Classification of the trajectories was based on their region of origin and the path that they followed to the western Pacific. *Jordan et al.* [2003] used the same source region classification to characterize the aerosol distribution in East

Asia and included examples and descriptions of the trajectories in each source region. *Jordan et al.* [2003] refers to the central region as "Channel."

[11] The data was further separated into three altitude ranges, <2 km, 2–7 km, and >7 km, representing the boundary layer, middle troposphere, and upper troposphere. The three bins reflect the aircraft's altitude at the sampling time. The ranges were chosen based on vertical distributions of O_3 and aerosols obtained by the DIAL instrument [*Browell et al.*, 2003]. The data was not evenly distributed across the five source regions during the time period of the measurements due to the altitudes flown by the DC-8. For example, the WSW region did not contain any boundary layer data, and the coastal region does not have data above ~4 km. Also, the trajectories that comprise the central region were constrained by mountains to the north and the Tibetan Plateau to the south. As a result, the central region does not have data >7 km because the high-altitude trajectories are not affected by the topography of this region [*Jordan et al.*, 2003].

4. Characterization of Flights 6–17

[12] This section discusses some general features of the observed trace gas distributions over the western Pacific for Flights 6–17, including measurements made during both constant altitude and spiral flight legs. The term "enhanced" is used to indicate when a species mixing ratio was greater than its Northern Hemisphere background mixing ratio. Measurements obtained during Flight 5, which was a transit flight from Hawaii to Guam, were used to estimate the background mixing ratios. Several
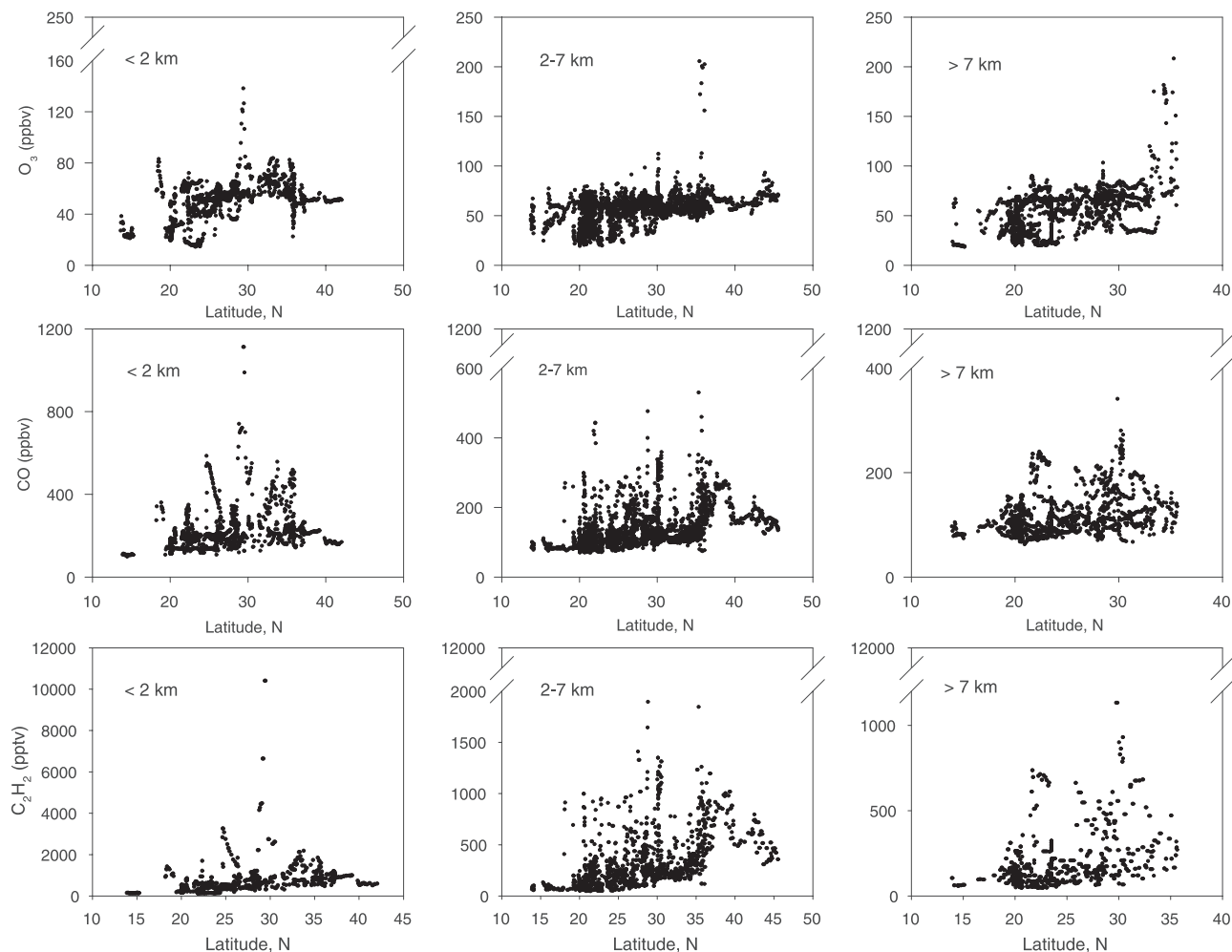
Figure 2. Latitudinal distribution of O_3, CO, and C_2H_2 mixing ratios for Flights 6−17 for three altitude ranges: <2, 2−7, and >7 km.

of the back trajectories from Flight 5 only traveled over the ocean indicating that the air masses were composed of clean, aged marine air, and thus should be fairly representative of springtime, Northern Hemispheric background air. Background was considered to be the lowest one third of measurements in each altitude range. Background mixing ratios for several gases are listed below. The first value corresponds to the background mixing ratio below 2 km, the second corresponds to 2−7 km, and the third number is the background above 7 km: CO = 90, 80, 74 ppbv, O_3 = 15, 20, 15 ppbv, C_2Cl_4 = 3, 2.5, 2 pptv, CH_3Cl = 530, 530, 520 pptv, C_2H_2 = 120, 65, 50 pptv, C_2H_6 = 650, 480, 420 pptv, C_3H_8 = 50, 20, 15 pptv, and SO_2 = 7, 20, 14 pptv.

[13] The latitudinal distribution of O_3 in the three altitude ranges over the western Pacific basin was relatively similar. The mean O_3 mixing ratio at all altitudes was ∼50−60 ppbv (Figure 2). The large peaks approaching 200 ppbv in the middle and upper altitudes occurred in air masses with a mix of stratospheric and polluted air. Coincident with the high O_3 were enhanced mixing ratios of CO (80−150 ppbv) indicative of a combustion influence in these air masses. As a result, the stratospheric influence could not be completely removed. The mean CO mixing ratio in the boundary

was ∼200 ppbv, and 100−130 ppbv in the middle and upper troposphere (Figure 2). This suggests that an anthropogenic influence was present at all altitudes over the western Pacific. The abnormally large peak in the boundary layer near 30°N was due to the Shanghai plume which will be discussed in more detail in a later section.

[14] The most significant outflow occurred in the boundary layer between 20 and 40°N latitude, which corresponds to surface outflow directly off of China, Japan and Korea. Several species, such as CO, CO_2, C_2H_2, C_2H_6, C_3H_8, and C_2Cl_4, exhibited enhanced mixing ratios between ∼30 and 45°N suggesting a general trend increasing with latitude (Figure 2, only CO and C_2H_2 shown). This feature was particularly noticeable in the middle altitudes. Several companion papers also concluded that the strongest outflow occurred in this midlatitude band [e.g., *Liu et al.*, 2003; *Vay e tal.*, 2003]. During PEM-West B, *Blake et al.* [1997] found a sharp transition at 25°N latitude with stronger outflow and larger mixing ratios for C_2H_6, C_2H_2, and C_2Cl_4 to the north, and this trend was most pronounced in the middle altitudes. Both the location of the major industrial areas and the strong outflow conditions in the late winter and spring at these latitudes were proposed to be responsible for the high mixing ratios.
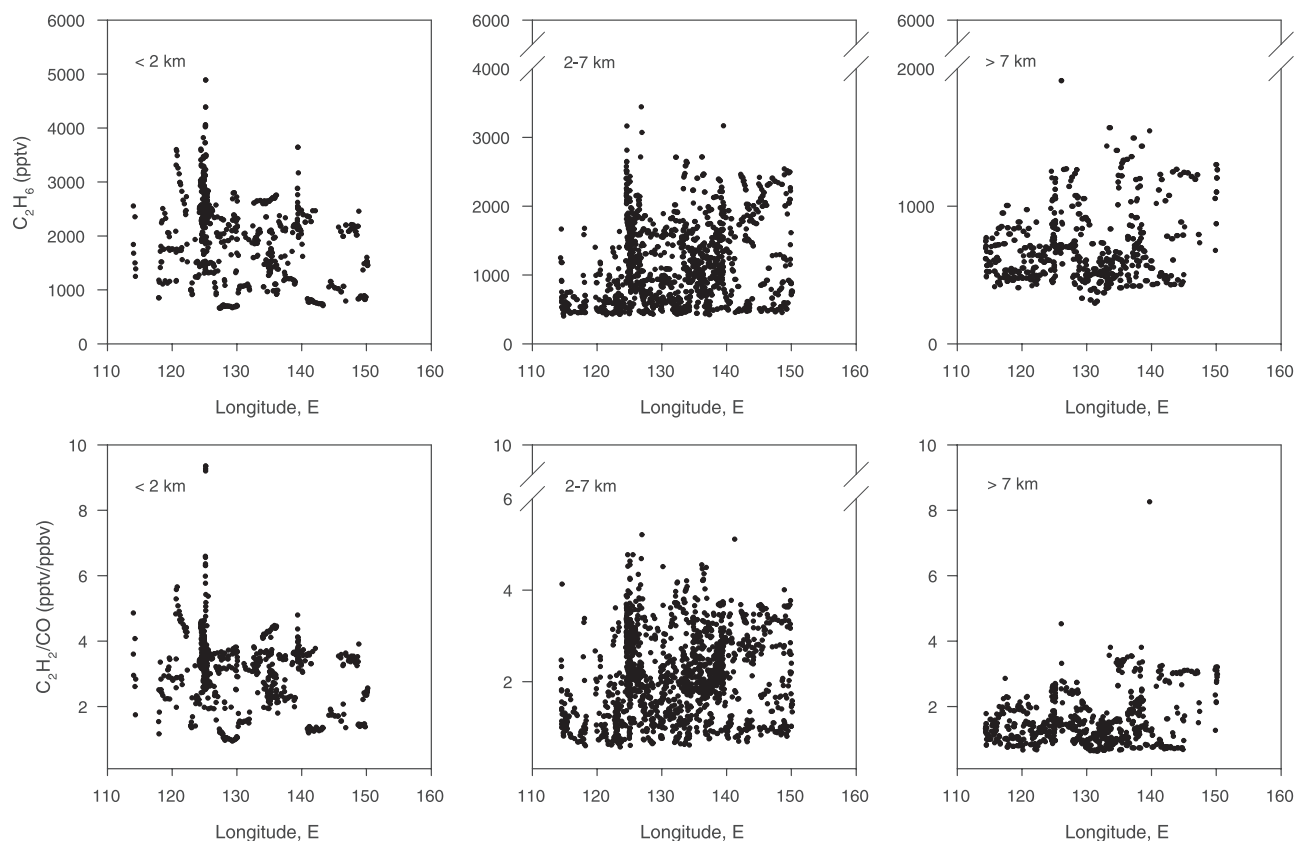
Figure 3. Longitudinal distribution of C_2H_6 mixing ratios and the C_2H_2/CO ratio for Flights 6–17 for <2, 2–7, and >7 km.

[15] An important finding of TRACE-P was that significant outflow was encountered in the middle and upper troposphere and as far east as 150°E longitude (Figure 3). This indicates that anthropogenic influences were not confined to surface regions close to the Asian continent and suggests that emissions were rapidly uplifted and transported over the western Pacific. CO, CO_2, SO_2, C_2Cl_4, CH_3Cl, and non-methane hydrocarbons (NMHCs), such as C_2H_2, C_2H_6, C_3H_8, C_2H_4, had enhanced mixing ratios in the free troposphere. For instance, at 150°E longitude, CO reached over 250 ppbv in the middle altitudes and ~200 ppbv at higher altitudes. SO_2 mixing ratios peaked at approximately 6000 pptv in the middle altitude range. Also, C_2H_6 reached ~3000 pptv and ~1500 pptv in the middle and upper troposphere, respectively (Figure 3). In addition, *Vay et al.* [2003] found that the most efficient continental outflow and that nearly 80% of the CO_2 flux from the Asian continent occurred in the middle troposphere between 35 and 40°N.

[16] The relative age of an air mass resulting from atmospheric processing (mixing and photochemistry) can be estimated because of the different reactivities of chemical species emitted during combustion. NMHCs with short lifetimes will be removed from an air mass before longer-lived species; thus the mixing ratio of the short-lived species will decrease more quickly and alter the ratio value [e.g., *McKeen and Liu*, 1993; *Smyth et al.*, 1996]. The C_2H_2/CO and C_3H_8/C_2H_6 ratios are used in this paper to indicate air mass processing. A higher ratio (i.e., $C_2H_2/CO > 3$, $C_3H_8/C_2H_6 > 0.3$) suggests that an air mass contains recent emissions (less than a few days old) while a lower ratio

(i.e. $C_2H_2/CO < 1$, $C_3H_8/C_2H_6 < 0.1$) is indicative of an aged air mass (~1 week old) [e.g., *Gregory et al.*, 1997].

[17] During TRACE-P, both recent and aged emissions reached the free troposphere and were transported into the central Pacific as indicated by the longitudinal distribution of the C_2H_2/CO (Figure 3) and C_3H_8/C_2H_6 ratios. At 150°E longitude, the C_2H_2/CO ratio had values as large as 4, and this was particularly noticeable in the middle altitude range. These results indicate that the combustion emissions were only 2 or 3 days old, implying rapid uplifting from the Asian continent and transport to these remote oceanic areas. The C_3H_8/C_2H_6 ratio demonstrated similar behavior and trends in its values. In each altitude range and at 150°E longitude, the C_3H_8/C_2H_6 ratio reached values of approximately 0.2 and higher.

5. Characterization of Air Mass Source Regions

[18] This section discusses and compares the characteristics of the five principal Asian source regions identified by analysis of backward trajectories. Atmospheric tracer species were used to determine which pollution sources contributed emissions to regional outflow. Elevated mixing ratios of CO and C_2H_2 are indicative of combustion sources [*Singh and Zimmerman*, 1992]. C_2Cl_4 is an industrial/urban tracer since its only known source is through anthropogenic activities [*Blake et al.*, 1996; *Wang et al.*, 1995]. In addition, CH_3Cl and HCN are good tracers of biomass burning [*Blake et al.*, 1996; *Singh et al.*, 2003; *Li et al.*, 2003]. Tables 1–5 present summary statistical information describing the chemical

Table 1. Mixing Ratios for Selected Species From the Central Source Region[a]

	<2 km						2−7 km					
Species	Mean	Median	Std. Dev.	Max	Min	N	Mean	Median	Std.Dev.	Max	Min	N
O_3	64	64	13	138	41	229	60	61	6	76	47	129
CO	303	264	153	1113	135	215	140	135	25	219	104	128
NO	73	48	77	399	0	211	14	11	11	64	2	82
NO_2	530	477	421	2926	8	184	55	51	38	177	0	71
NO_y	2430	1726	2249	13487	222	228	297	276	150	938	65	129
HNO_3	1323	833	1293	7412	222	229	202	169	110	938	106	120
PAN	1225	888	1014	4264	2	102	194	175	69	364	118	41
SO_2	4172	2621	4428	30736	353	205	80	65	64	284	10	91
CO_2	378	377	3	392	374	199	374	374	1	376	372	118
H_2O_2	567	446	441	2137	20	122	741	535	552	1725	134	49
CH_3OOH	98	88	50	293	36	107	228	225	108	482	104	35
CH_2O	2640	1690	2884	9824	208	35	85	82	19	122	61	17
C_2H_6	2695	2540	662	4888	1396	110	1415	1334	221	1968	1125	44
C_2H_4	396	106	681	3052	4	108	27	19	22	93	3	44
C_2H_2	1465	860	1639	10403	308	110	339	313	107	645	209	44
C_3H_8	1010	822	586	3774	271	110	308	279	96	540	184	44
C_6H_6	431	240	549	3101	61	110	64	62	25	147	28	44
i-C_4H_{10}	205	125	231	1345	31	110	40	39	16	83	15	44
n-C_4H_{10}	290	209	229	1384	46	110	67	58	30	151	27	44
CH_4	1856	1855	33	1983	1788	208	1797	1794	13	1837	1767	118
C_2Cl_4	18	12	19	123	8	110	6	6	2	10	4	44
CCl_4	104	100	11	162	98	110	99	99	1	102	97	44
CH_3CCl_3	43	41	5	66	40	110	40	40	0	41	39	44
CH_3Cl	654	559	239	1677	530	110	568	563	23	643	542	44
CH_3Br	10	9	4	29	8	110	9	9	0.27	9	8	44
CFC-11	264	262	7	293	259	110	259	259	2	262	255	44
CFC-12	543	540	12	615	534	110	535	535	3	543	528	44
CFC-113	81	80	5	113	77	110	79	79	1	80	78	44
C_2H_2/CO	3.87	3.37	1.34	9.35	2.24	102	2.40	2.35	0.40	3.82	1.91	43
C_3H_8/C_2H_6	0.35	0.33	0.09	0.77	0.19	110	0.21	0.21	0.04	0.31	0.15	44

[a]Mixing ratios are given in parts per trillion by volume except for O_3, CO, and CH_4 which are in parts per billion by volume and for CO_2 which is in parts per million by volume. The C_2H_2/CO ratio is in parts per trillion by volume/parts per billion by volume.

composition of the five source regions. This information is used in our discussion of each of the five source regions.

5.1. Central

[19] The most striking feature of the central region was the Shanghai plume which was sampled in the boundary layer (∼0.3 km) during Flight 13 over the Yellow Sea (Figure 4). Several species had their highest mixing ratios measured during the entire mission in this plume (Table 1), including CO, SO_2, C_2H_2, C_2H_6, C_2H_4, C_3H_8, CH_2O, C_2Cl_4, CCl_4, CH_3CCl_3, CH_3Cl, HNO_3, PAN, and NO_y (NO_y = NO + NO_2 + HNO_3 + PAN + PPN + C_1-C_5 alkyl nitrates). For example, CO mixing ratios peaked at ∼1100 ppbv, C_2H_2 at ∼10,000 pptv, SO_2 at ∼31,000 pptv, C_2Cl_4 at 123 pptv, and CH_3Cl at ∼1700 pptv. Aerosol Ca^{+2} and NO_3^- were also significantly enhanced in the boundary layer indicating a strong dust and anthropogenic influence [*Jordan et al.*, 2003]. The Shanghai plume was largely composed of recent combustion emissions that were less than 1 day old (maximum C_2H_2/CO = 9.4, C_3H_8/C_2H_6 = 0.77). The observed composition of the plume was most likely quite similar to its original composition. Photochemical species, such as O_3, PAN, HNO_3, CH_3OOH, and H_2O_2, were also enhanced. For example, O_3 reached ∼140 ppbv while PAN peaked near 4300 pptv. These high levels indicate significant photochemical activity even at this time of the year. Correlations of O_3 and CO (r^2 = 0.82) and O_3 and PAN (r^2 = 0.69) were fairly robust and suggested that O_3 and PAN were photochemically produced from combustion derived precursor gases in the outflow. The strong correlation between O_3 and CO reflects the recent emission inputs into the Shanghai plume where dilution and mixing processes had not acted to significantly alter the overall composition of the plume. O_3 and CO were poorly correlated in the other four source regions, where the emissions were clearly more than 1 day old. *Simpson et al.* [2003] discuss the chemistry and production of C_2-C_5 alkyl nitrates in Asian outflow and concluded that the Shanghai plume contained very fresh emissions of these species and that dilution was not a significant factor affecting the observed plume composition.

[20] Pollution plumes from other urban regions around the world show enhancements in many of the same anthropogenic species, specifically CO, NMHCs, and halocarbons. However, these enhancements occur in varying degrees compared to the Shanghai plume. For example, NMHC mixing ratios in the southeast U.S. and Houston, Texas have been found to be substantially higher than in the Shanghai plume [e.g., *Kang et al.*, 2001]. The mixing ratios of several hydrocarbons (e.g., C_2H_6, C_3H_8, C_2H_2, C_6H_6) have been found to be factors of ∼2−50 higher in Mexico City [*Blake and Rowland*, 1995]. Also, C_2H_6, C_2H_2, C_3H_8, C_6H_6, and CO were observed to be approximately a factor of 2 larger in London in the winter than the maximum values of these species observed in the Shanghai plume [*Derwent et al.*, 1995]. A notable difference between the Shanghai plume and other urban regions is the large influence from biofuel emissions most likely reflecting their use for cooking and heating in East Asia. C_3H_8, C_2H_2, C_2H_6, C_6H_6, i-C_4H_{10}, and n-C_4H_{10} mixing ratios observed in South Korea were fairly comparable with the Shanghai

Table 2. Mixing Ratios of Selected Species From the Coastal Source Region[a]

Species	<2 km						2–4 km					
	Mean	Median	Std. Dev.	Max	Min	N	Mean	Median	Std. Dev.	Max	Min	N
O_3	41	43	14	83	15	290	58	60	6	69	43	111
CO	201	166	107	586	124	264	151	132	47	272	107	83
NO	7	2	15	79	0	221	23	17	20	110	5	94
NO_2	41	13	89	503	0	195	35	33	22	137	6	65
NO_y	541	386	525	3267	56	283	431	475	260	1096	24	110
HNO_3	439	322	365	2120	128	267	368	326	169	876	135	95
PAN	207	19	336	1065	1	104	142	115	126	412	15	51
SO_2	207	48	377	1554	4	105	27	21	19	120	10	38
CO_2	376	375	3.5	389	373	233	374	374	1.1	376	372	84
H_2O_2	1243	1176	611	3179	339	108	1404	1553	591	3093	416	58
CH_3OOH	470	351	359	1535	53	100	269	280	117	531	84	55
CH_2O	763	461	797	3553	92	90	265	245	128	488	55	32
C_2H_6	1498	1353	716	3598	669	105	1085	929	336	1974	793	39
C_2H_4	208	9	452	1794	3	93	30	22	25	87	3	23
C_2H_2	665	384	749	3264	125	105	376	255	222	908	181	39
C_3H_8	375	211	448	2069	27	105	171	131	89	375	65	39
C_6H_6	189	79	272	1207	30	105	77	42	55	185	27	39
$i-C_4H_{10}$	94	32	160	738	9	89	23	12	20	65	4	39
$n-C_4H_{10}$	121	38	211	1030	4	93	36	16	30	100	7	39
CH_4	1816	1808	34	1915	1735	241	1779	1776	11	1831	1761	72
C_2Cl_4	9	8	6	32	3	105	5	5	2	11	3	39
CCl_4	102	100	6	127	97	105	100	100	1	102	99	39
CH_3CCl_3	41	41	3	54	39	105	40	40	1	41	39	39
CH_3Cl	638	580	176	1333	522	105	589	575	32	662	549	39
CH_3Br	10	9	2	18	8	105	9	9	0.43	10	8	39
CFC-11	262	261	4	277	256	105	261	261	1	264	259	39
CFC-12	540	538	6	559	532	105	539	538	3	544	534	39
CFC-113	80	80	1	85	77	105	80	80	1	81	79	39
C_2H_2/CO	2.46	2.28	1.19	5.66	0.94	94	2.27	1.91	0.71	3.94	1.66	31
C_3H_8/C_2H_6	0.19	0.16	0.12	0.58	0.04	105	0.15	0.13	0.05	0.24	0.08	39

[a]Mixing ratios are given in parts per trillion by volume except for O_3, CO, and CH_4 which are in parts per billion by volume and for CO_2 which is in parts per million by volume. The C_2H_2/CO ratio is in parts per trillion by volume/parts per billion by volume.

Table 3. Mixing Ratios of Selected Species From the SE Source Region[a]

Species	<2 km						2–7 km						>7 km					
	Mean	Median	Std. Dev.	Max	Min	N	Mean	Median	Std. Dev.	Max	Min	N	Mean	Median	Std. Dev.	Max	Min	N
O_3	39	40	3	43	27	25	52	57	13	72	27	244	39	32	17	70	18	620
CO	208	205	18	254	157	25	123	88	69	331	74	231	98	88	27	223	67	557
NO							16	15	12	130	1	171	92	47	157	805	9	377
NO_2							31	26	16	65	5	89	14	11	11	48	0	240
NO_y	795	796	43	884	730	25	369	301	325	1439	5	219	172	125	177	1158	6	589
HNO_3	784	783	47	884	713	25	336	238	230	1352	100	174	86	66	66	320	3	502
PAN	17	17	8	27	3	9	159	86	186	660	8	98	62	54	56	238	6	287
SO_2	23	20	11	45	7	16	32	23	56	415	6	102	38	21	51	284	10	93
CO_2	376	376	0.65	377	374	23	372	371	2	379	370	222	372	371	1	374	370	279
H_2O_2	5660	5699	508	6199	4857	9	739	266	1019	5391	48	96	164	109	154	686	15	210
CH_3OOH	1351	1331	223	1791	1121	10	257	216	195	1083	30	71	114	103	65	340	29	125
CH_2O	346	300	114	516	268	4	162	127	108	406	53	36	248	143	286	1138	56	50
C_2H_6	1182	1155	104	1412	1105	7	737	528	405	1775	422	88	594	514	194	1270	370	279
C_2H_4	6	6	1	8	5	5	31	14	38	132	2	43	16	5	31	160	3	84
C_2H_2	459	456	82	627	369	7	252	93	321	1210	48	88	129	89	105	609	47	279
C_3H_8	123	112	18	156	109	7	81	35	108	430	15	88	54	33	49	257	11	279
C_6H_6	88	86	16	118	70	7	53	13	84	328	3	86	18	11	21	124	3	259
$i-C_4H_{10}$	14	17	5	19	7	7	28	11	32	103	3	35	12	7	10	44	3	122
$n-C_4H_{10}$	18	19	6	24	8	7	28	6	41	144	3	53	14	8	15	66	3	163
CH_4	1800	1799	5	1809	1786	25	1762	1754	28	1836	1690	194	1757	1755	13	1799	1713	456
C_2Cl_4	5	5	0	5	4	7	4	2	3	15	1	88	2	2	1	6	1	279
CCl_4	99	100	1	100	98	7	99	99	1	103	97	88	98	98	1	101	95	279
CH_3CCl_3	39	40	1	40	38	7	40	39	2	45	37	88	39	39	1	41	38	279
CH_3Cl	620	624	23	654	588	7	582	567	41	709	536	88	569	561	32	641	525	279
CH_3Br	9	9	0	9	8	7	8	8	1	11	8	88	8	8	0	9	7	279
CFC-11	260	260	1	261	259	7	260	260	2	268	256	88	258	258	2	263	254	279
CFC-12	536	536	1	537	534	7	536	537	4	552	528	88	534	534	4	543	525	266
CFC-113	79	79	1	80	78	7	79	79	1	82	77	88	79	79	1	81	77	279
C_2H_2/CO	2.26	2.24	0.23	2.51	1.82	7	1.50	1.01	0.98	4.13	0.63	83	1.15	1.01	0.47	2.74	0.63	250
C_3H_8/C_2H_6	0.10	0.10	0.01	0.12	0.09	7	0.08	0.06	0.05	0.24	0.03	88	0.08	0.06	0.04	0.20	0.02	279

[a]Mixing ratios are given in parts per trillion by volume except for O_3, CO, and CH_4 which are in parts per billion by volume and for CO_2 which is in parts per million by volume. The C_2H_2/CO ratio is in parts per trillion by volume/parts per billion by volume.

Table 4. Mixing Ratios of Selected Species From the NNW Source Region[a]

Species	<2 km						2–7 km						>7 km					
	Mean	Median	Std. Dev.	Max	Min	N	Mean	Median	Std. Dev.	Max	Min	N	Mean	Median	Std. Dev.	Max	Min	N
O_3	55	54	7	67	36	399	62	60	17	206	48	491	131	151	53	208	59	25
CO	204	207	25	266	136	368	145	126	46	420	74	443	103	105	9	118	88	25
NO	61	18	136	1450	0	297	33	10	78	465	0	402	56	55	28	97	22	17
NO_2	463	72	766	3349	0	190	51	27	63	664	1	402	23	23	13	40	5	17
NO_y	940	597	881	5115	12	391	397	260	397	3341	10	492	585	782	390	1230	88	24
HNO_3	447	436	195	1198	63	375	189	120	229	2028	49	452	456	543	349	1099	41	25
PAN	505	514	326	1422	1	160	293	193	229	998	89	229	116	124	28	151	80	16
SO_2	517	272	559	2821	4	328	403	42	1038	6989	7	398	31	24	17	70	12	18
CO_2	377	376	2	387	374	389	374	374	1.6	380	370	466	372	372	0.9	373	371	19
H_2O_2	543	425	442	2276	22	158	440	397	308	1058	30	210	96	90	59	201	22	10
CH_3OOH	169	111	172	1091	25	124	208	138	139	597	28	180	76	75	26	109	45	4
CH_2O	723	739	395	1935	83	113	292	138	400	1877	50	44	160	176	42	188	99	4
C_2H_6	2356	2353	407	3607	1276	135	1670	1646	411	2813	641	216	882	916	175	1076	597	14
C_2H_4	150	101	180	1228	19	134	38	15	59	318	3	179	5	5	2	8	3	8
C_2H_2	756	757	166	1205	268	135	398	304	211	1098	117	216	179	164	34	238	138	14
C_3H_8	859	804	310	1907	194	135	446	413	199	1115	96	216	149	133	60	232	71	14
C_6H_6	182	175	50	326	68	135	76	52	61	308	3	216	19	21	7	25	7	8
i-C_4H_{10}	144	130	71	386	20	135	60	52	35	189	8	216	7	6	3	12	4	14
n-C_4H_{10}	247	213	130	681	21	135	107	95	62	344	14	214	14	12	4	23	7	14
CH_4	1843	1841	17	1897	1803	318	1806	1802	22	1875	1750	438	1761	1760	11	1779	1744	25
C_2Cl_4	12	12	2	21	6	135	8	7	3	18	2	216	2	2	1	4	1	14
CCl_4	100	100	1	102	98	135	99	99	1	103	90	216	95	96	2	97	92	14
CH_3CCl_3	42	42	1	45	40	135	40	40	1	43	38	216	38	38	1	39	36	14
CH_3Cl	552	553	17	589	518	135	552	547	21	618	514	216	544	545	12	559	523	14
CH_3Br	9	9	1	18	9	135	9	9	1	11	8	216	9	9	0	9	8	14
CFC-11	262	262	2	269	257	135	260	260	3	266	245	216	253	255	5	258	244	14
CFC-12	540	540	3	549	530	135	537	538	4	550	518	216	530	532	8	537	517	14
CFC-113	80	80	1	82	78	135	79	79	1	82	75	216	78	77	1	79	76	14
C_2H_2/CO	3.60	3.56	0.47	4.61	2.80	117	2.54	2.37	0.56	4.02	1.00	172	1.72	1.62	0.25	2.19	1.44	14
C_3H_8/C_2H_6	0.35	0.36	0.07	0.53	0.15	135	0.26	0.25	0.07	0.49	0.12	217	0.16	0.15	0.04	0.22	0.12	14

[a]Mixing ratios are given in parts per trillion by volume except for O_3, CO, and CH_4 which are in parts per billion by volume and for CO_2 which is in parts per million by volume. The C_2H_2/CO ratio is in parts per trillion by volume/parts per billion by volume.

Table 5. Mixing Ratios of Selected Species From the WSW Source Region[a]

Species	2–7 km						>7 km					
	Mean	Median	Std. Dev.	Max	Min	N	Mean	Median	Std. Dev.	Max	Min	N
O_3	64	65	10	91	29	145	62	66	15	120	26	625
CO	110	108	17	175	78	136	134	121	48	281	70	556
NO	44	51	31	119	7	60	93	82	55	285	9	445
NO_2	45	43	19	83	10	52	29	24	21	149	2	358
NO_y	322	235	349	2257	5	140	297	245	211	1138	3	619
HNO_3	210	131	312	1987	33	128	121	100	83	762	25	518
PAN	187	187	63	341	78	67	268	181	186	699	44	246
SO_2	72	26	88	298	10	26	51	28	100	569	7	151
CO_2	372	372	1	373	371	131	372	372	2	376	369	521
H_2O_2	415	255	314	1091	94	60	205	193	125	589	22	215
CH_3OOH	170	195	70	286	25	47	120	98	91	540	25	141
CH_2O	262	189	272	1166	56	16	266	218	188	729	54	59
C_2H_6	824	893	191	1242	451	56	801	731	294	1569	295	260
C_2H_4	17	14	11	50	3	33	41	26	38	129	3	140
C_2H_2	211	190	108	602	81	56	291	208	219	930	47	260
C_3H_8	110	120	54	202	19	56	93	77	63	259	12	260
C_6H_6	31	24	23	107	7	56	46	30	43	179	3	223
i-C_4H_{10}	11	11	5	23	3	49	16	13	11	41	3	166
n-C_4H_{10}	19	20	9	36	3	51	21	14	18	65	3	203
CH_4	1767	1771	13	1794	1726	136	1771	1772	19	1831	1694	482
C_2Cl_4	3	3	1	6	2	56	3	2	2	12	0	260
CCl_4	98	98	1	101	96	56	98	98	2	101	87	260
CH_3CCl_3	39	39	1	41	37	56	39	39	2	41	31	260
CH_3Cl	568	566	19	621	538	56	595	588	29	668	543	260
CH_3Br	8	8	0	9	8	55	8	8	0.45	10	8	260
CFC-11	259	259	2	263	255	56	258	257	2	264	253	260
CFC-12	535	535	4	543	527	56	534	534	3	544	527	258
CFC-113	79	79	1	87	77	56	79	79	1	81	73	260
C_2H_2/CO	1.88	1.82	0.63	4.49	0.98	52	1.95	1.59	0.80	3.81	0.67	229
C_3H_8/C_2H_6	0.13	0.13	0.04	0.21	0.04	56	0.10	0.10	0.04	0.21	0.03	260

[a]Mixing ratios are given in parts per trillion by volume except for O_3, CO, and CH_4 which are in parts per billion by volume and for CO_2 which is in parts per million by volume. The C_2H_2/CO ratio is in parts per trillion by volume/parts per billion by volume.
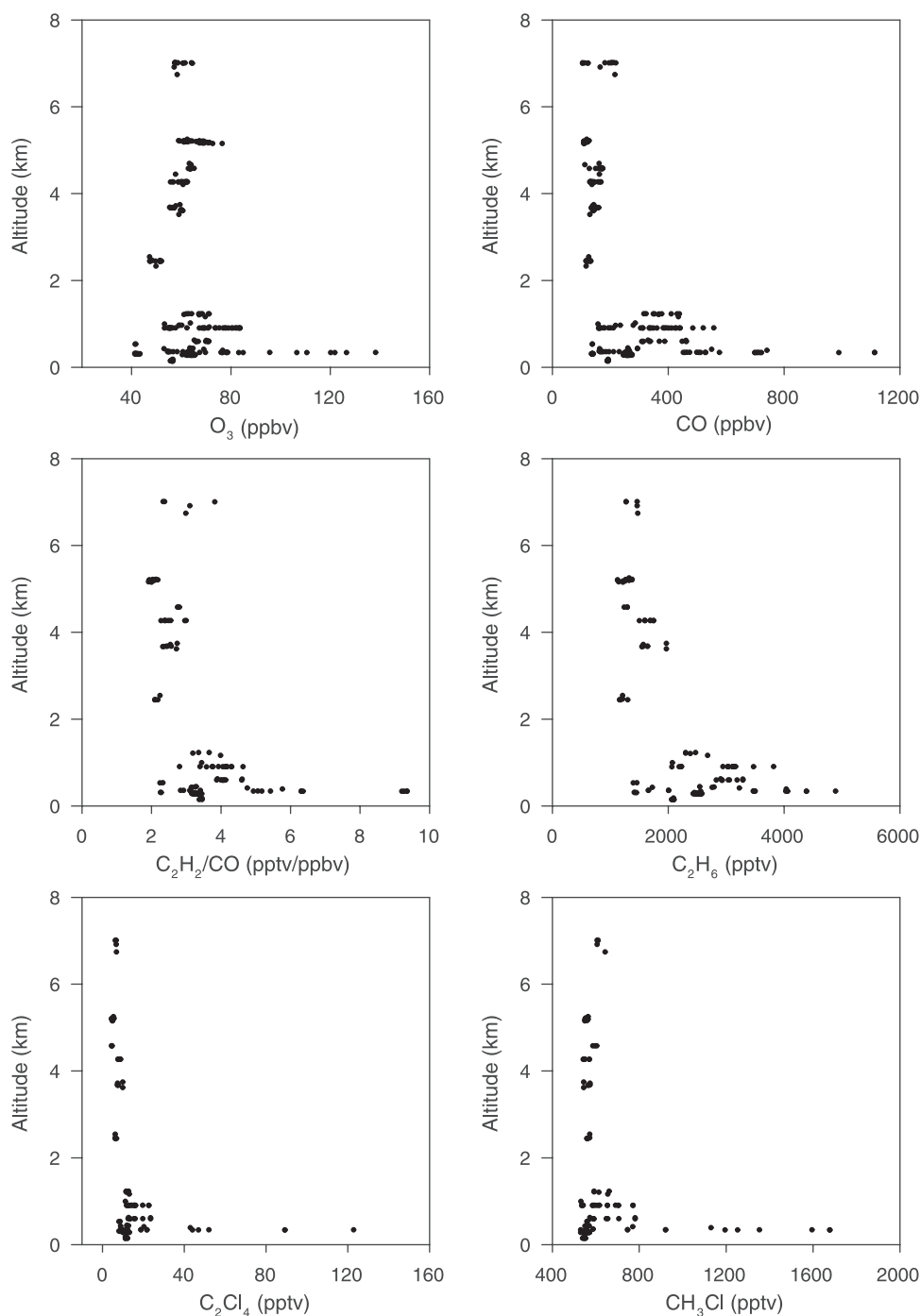
Figure 4. Vertical distributions of selected species in air masses originating in the Central source region.

plume [*Na et al.*, 2003]. These comparisons for polluted regions around the world suggest that the Shanghai plume is fairly representative of the magnitude of pollutants being transported from these large population centers.

[21] In the boundary layer outflow of the central region, CO was strongly correlated with C_2H_2, C_2H_4, and C_2H_6 ($r^2 \geq 0.86$). CO and C_2H_2 were also correlated with C_2Cl_4 ($r^2 = 0.77$ and 0.96, respectively) and with CH_3Cl ($r^2 = 0.81$ and 0.90, respectively). These results indicate that the outflow contained a complex mixture of fresh and processed emissions from combustion, industrial activities, and biomass/biofuel burning. This makes it difficult to distinguish

between fossil fuel and biofuel emissions. The strong correlations, particularly with C_2H_2, were dominated by the emissions sampled directly from the Shanghai plume. Additional tracers have been identified which can specifically distinguish between Chinese (halon-1211) and Japanese/ Korean (CH_3Br) emissions [*Blake et al.*, 2003]. Correlations between CO, C_2H_2, and C_3H_8 with H-1211 ($r^2 = 0.72-0.93$) were stronger than the correlations with CH_3Br ($r^2 = 0.67-0.76$). As expected, these results suggest a stronger influence from Chinese sources in the boundary layer.

[22] Above the boundary layer, mixing ratios of most species were decreased significantly. The median CO and
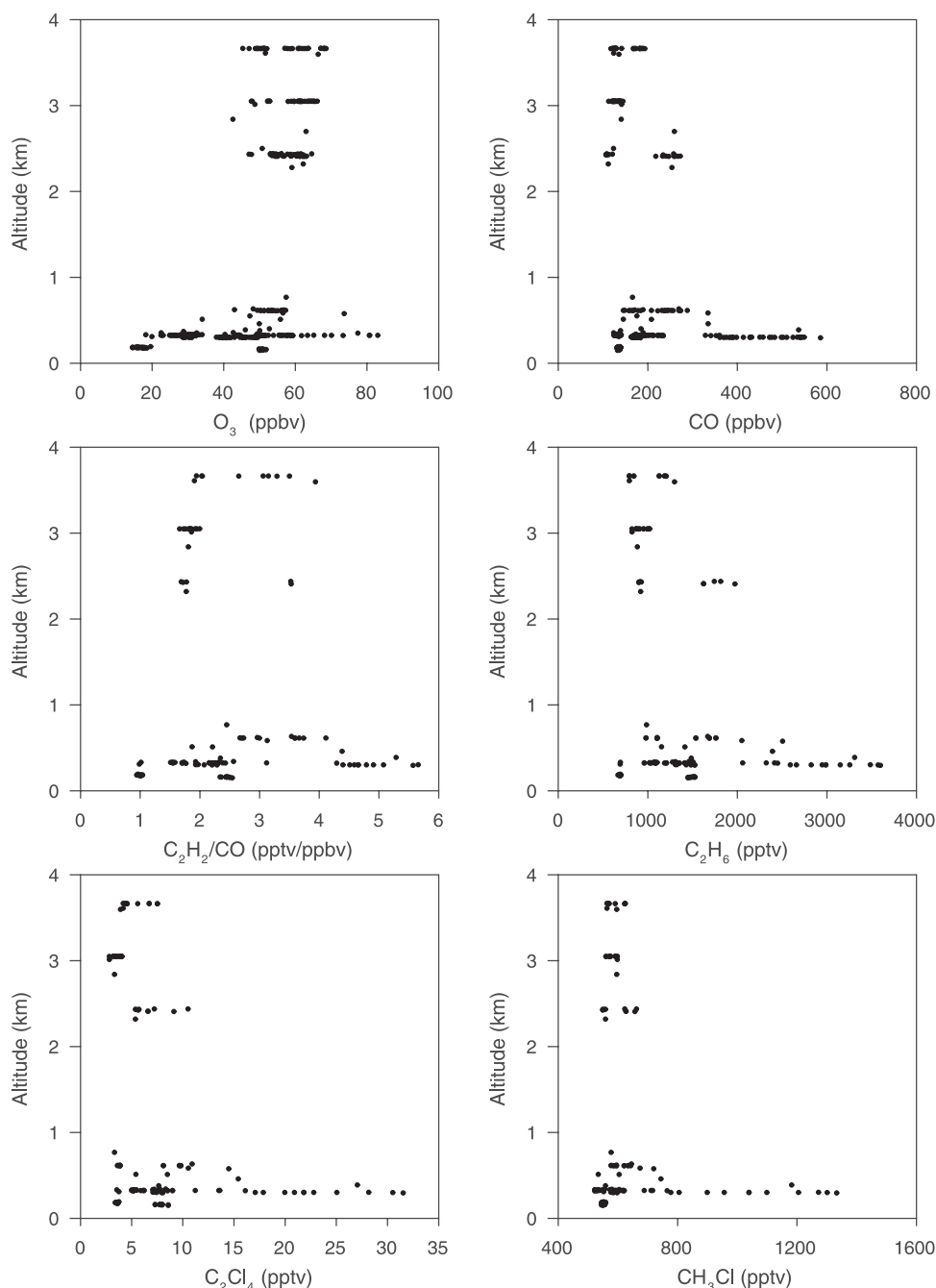
Figure 5. Vertical distributions of selected species in air masses originating in the Coastal source region.

NMHC mixing ratios were at least a factor of 2–3 lower in the middle altitudes compared to the boundary layer but they were still enhanced substantially above background levels. The hydrocarbon ratios were lower due to a lack of recent emission inputs and additional air mass processing and dilution. Correlations of CO and C_2H_2 with CH_3Cl ($r^2 =$ 0.83 and 0.58, respectively) indicate an influence from combustion and, in particular, biomass/biofuel burning emissions in the middle altitudes.

5.2. Coastal

[23] The middle altitudes of the coastal region only reflect data collected at 2–4 km while observations were available

for the other four regions from 2 to 7 km. Air masses in the coastal region had short transport distances to the western Pacific and apparently underwent minimal vertical uplifting. Aside from the differences in the air mass transport patterns and the strong dust influence in the central region [*Jordan et al.*, 2003], the chemistry of the central and coastal regions was essentially the same. The composition of the boundary layer in these two regions was directly influenced by recent emissions from anthropogenic activities in East Asia. Mixing ratios of CO, NMHCs, C_2Cl_4, and CH_3Cl were at least a factor of 3 higher than background (Figure 5, Table 2). Furthermore, O_3, PAN, NO_x, HNO_3, H_2O_2, and CH_3OOH were enhanced, suggestive of relatively recent photochem-

ical processing. This is supported by the strong correlation of CO and C_2H_2 with PAN ($r^2 \sim 0.85$). Recent (~ 1 day old) combustion inputs were present in the boundary layer outflow ($C_2H_2/CO \sim 5$ and $C_3H_8/C_2H_6 \sim 0.5$) along with extensively processed air. CO_2 and CH_4 were also enhanced in the boundary layer, and they were correlated with CO and C_2H_2 ($r^2 > 0.8$) suggesting an anthropogenic rather than biogenic source. In addition, CO_2 and CH_4 were correlated with combustion species ($r^2 > 0.6$) in the altitude ranges where outflow occurred in the other four source regions. *Vay et al.* [2003] analyzed eleven pollution plumes with $CO_2 > 380$ ppmv and $CO > 250$ ppbv and concluded that anthropogenic sources were responsible for the enhancements followed by frontal lifting associated with mid-latitude cyclones.

[24] In the middle altitudes, species mixing ratios decreased substantially, similar to those from the central region. Species, such as CO, C_2H_6, C_2H_4, C_2Cl_4, and CH_3Cl, were a factor of 2 or 3 lower compared to their maximum mixing ratios in the boundary layer. O_3, PAN, and H_2O_2 exhibited enhancements again showing significant photochemical processing. CO and C_2H_2 were well correlated with industrial tracer species, such as C_2Cl_4 ($r^2 > 0.91$ below 2 km and $r^2 \sim 0.7$ above 2 km). As found in the central region, CO and C_2H_2 were strongly correlated with CH_3Cl ($r^2 \geq 0.87$) in both altitude ranges. O_3 levels are often high in air masses containing aged biomass emissions [*Tang et al.*, 2003]. Biomass/biofuel burning may therefore explain the enhanced O_3 (~ 80 ppbv) observed in the boundary layer. Also, a combination of emissions from both Chinese and Japanese/Korean sources appear to be important as indicated by the strong correlations of CO, C_2H_2, C_2H_6, and C_3H_8 with both H-1211 and CH_3Br ($r^2 > 0.78$) in the boundary layer.

5.3. Southeast

[25] The SE region was characterized by two principal outflow regions, ~ 3 and 10 km (Figure 6). The outflow plume at 10 km altitude was especially impressive, with mixing ratios of CO exceeding 200 ppbv, C_2H_6 above 1000 pptv, and enhanced hydrocarbon ratios ($C_2H_2/CO \sim 3$ and $C_3H_8/C_2H_6 \sim 0.2$) (Table 3). Both outflow plumes had enhancements in CO, SO_2, NO_y, NMHCs, CH_3Cl, C_2Cl_4, CH_3CCl_3, and CCl_4. In the high-altitude outflow, water-soluble species, such as HNO_3, H_2O_2, and CH_3OOH, were not enhanced. In air masses that have recently been influenced by wet convection, the CH_3OOH/H_2O_2 ratio is usually >1 due to the greater solubility of H_2O_2 which is preferentially scavenged by precipitation [*Heikes*, 1992]. At high altitude, the CH_3OOH/H_2O_2 ratio was >1, suggesting that wet convection lifted the emis-sions from the surface. This is consistent with the results from *Liu et al.* [2003] who suggested that the La Nina conditions during spring 2001 resulted in more frequent and stronger convection in SE Asia. This could be responsible for outflow of biomass burning emissions at high altitude. *Fuelberg et al.* [2003] also discuss the La Nina conditions during spring 2001 and its impact on transport patterns. O_3 had a wide range of mixing ratios varying from 20 to 70 ppbv at all altitudes. The enhanced O_3 mixing ratios at high altitude may be attributed to photochemical production from the uplifted biomass burning emissions. Extensively processed air

masses containing background air with low hydrocarbon ratios were also encountered above 2 km.

[26] The highest mixing ratios of H_2O_2 and CH_3OOH originated from the SE source region at altitudes of up to ~ 3 km. The median mixing ratios of H_2O_2 and CH_3OOH in the boundary layer were a factor of 4–15 larger than the medians in the other three source regions that had boundary layer data (i.e., central, coastal, NNW). Areas affected by significant biomass burning outflow, such as over the South Atlantic, have been found to contain considerably enhanced mixing ratios of H_2O_2 and CH_3OOH due to efficient photochemical production [*Talbot et al.*, 1996b; *Heikes et al.*, 1996]. Mixing ratios of NO_2, PAN, and HNO_3 were enhanced in the 3 km outflow, but NO was not enhanced presumably due to conversion to other reactive nitrogen species. This indicates that combustion was a significant source of reactive nitrogen in the Asian outflow.

[27] An anthropogenic influence was apparent in all three altitude ranges, with the strongest correlations found in the middle altitudes where CO was highly correlated with C_2H_2, C_2H_6, C_2Cl_4, and CH_3Cl ($r^2 \geq 0.89$). CH_3Cl has also been found to have an oceanic source [*Khalil et al.*, 1999] which may have made a minor contribution to the enhancements observed in the SE, central, and coastal regions. However, the correlations with the combustion species in these regions argue strongly for an anthropogenic source of CH_3Cl. Furthermore, biomass burning has been found to be a larger source of CH_3Cl than the ocean [*Lobert et al.*, 1999; *Khalil et al.*, 1999]. HCN has also been proposed to be a good tracer of biomass burning [*Singh et al.*, 2003; *Li et al.*, 2003]. Correlations of CH_3Cl, CO, C_2H_6, and C_2H_2 with HCN ($r^2 \geq 0.7$) are relatively strong providing further evidence of a significant impact from biomass burning in the SE region. Furthermore, it is likely that biomass burning made a large contribution because spring is the dry season in Asia and extensive biomass burning occurs at this time of year in India and SE Asia [e.g., *Bey et al.*, 2001; *Blake et al.*, 1997]. Several companion papers have also found evidence of substantial biomass burning emissions being transported from SE Asia. For instance, *Heald et al.* [2003] concluded that biomass burning was responsible for approximately 30% of the CO emissions south of 30°N. *Carmichael et al.* [2003a] also found that biomass burning emissions were transported from SE Asia above 2 km and below 30°N.

5.4. North-Northwest

[28] The vertical distributions for the NNW region show that outflow occurred at several altitudes between 2 and 8 km with several species exhibiting a general decreasing trend with altitude (Figure 7). Mixing ratios of CO, C_2Cl_4, and NMHCs decreased by factors of 3–4 from the boundary layer to the upper troposphere (Table 4). NO was enhanced (465 pptv) at ~ 7.5 km with coincident enhancements in several species, such as CO, C_2H_6, C_2H_2, CH_3Cl, and C_2Cl_4, suggesting that recent surface emissions were lifted to this altitude. The composition of the upper troposphere of the NNW region was influenced by a mixture of stratospheric and surface level air. O_3 and CO were both enhanced with mixing ratios of ~ 100 ppbv and higher. Also, the air masses were freshest at low altitude,
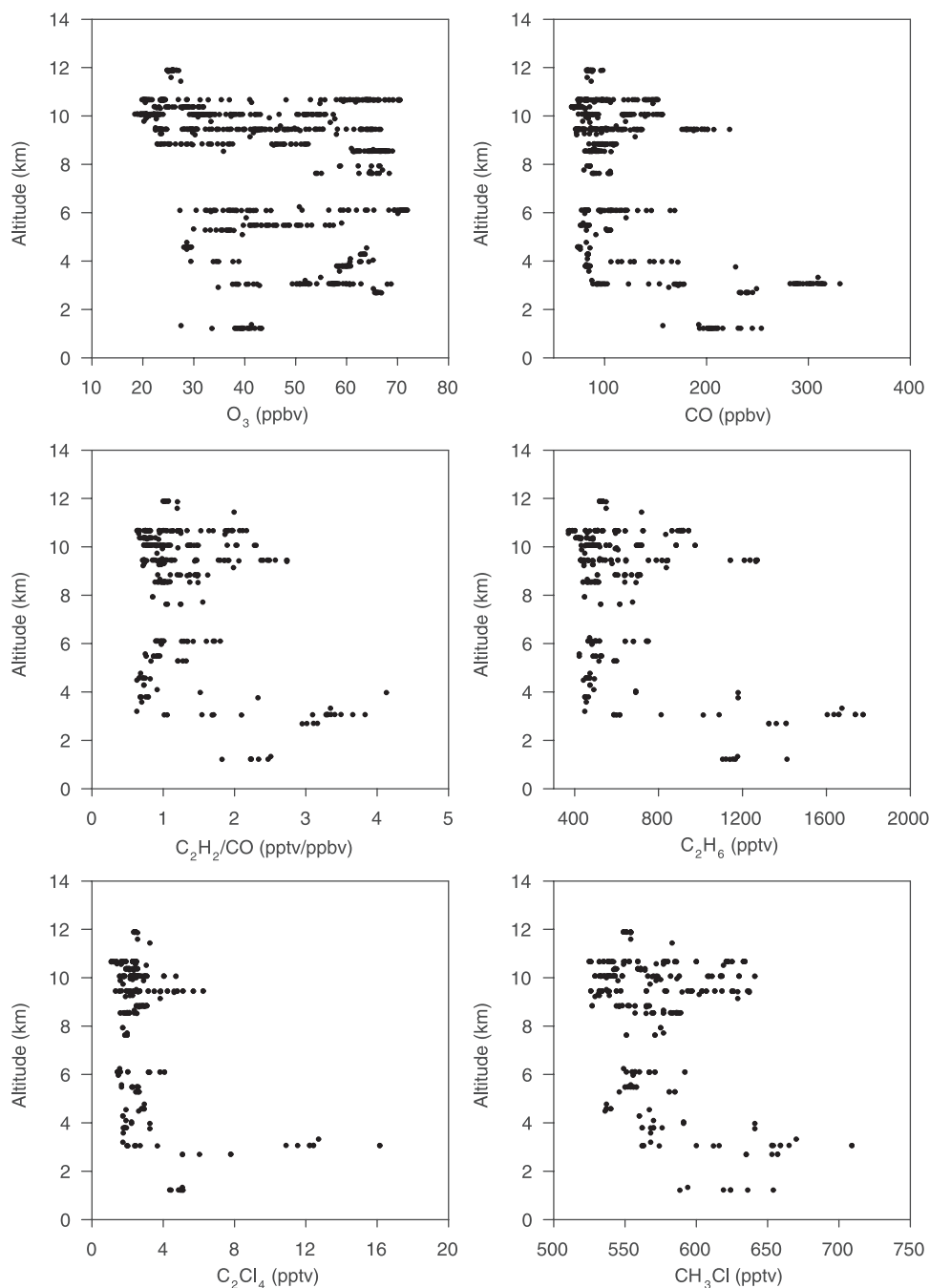
Figure 6. Vertical distributions of selected species in air masses originating in the Southeast source region.

and the relative age generally increased with altitude reflecting both stratospheric and aged surface emissions at the highest altitudes.

[29] Aged and diluted industrial and biomass/biofuel burning emissions were mixed with recent combustion emissions in the boundary layer. CO was weakly correlated with C_2Cl_4 and CH_3Cl ($r^2 < 0.3$) below 2 km, however, correlations of CO and C_2H_6 with C_2H_2 ranged from $r^2 = 0.74$ to 0.92 at low and middle altitudes. Emissions from industrial activity impacted the middle altitudes where CO and C_2H_2 were fairly well correlated with C_2Cl_4 ($r^2 = 0.68$ and 0.84, respectively).

[30] The presence of middle and high altitude outflow in the NNW, SE, and WSW regions undoubtedly reflects the longer transport distance for air masses which allows uplift and entrainment of continental emissions. Furthermore, these air masses may contain more processed and diluted emissions because of the long distance from source inputs. The relatively strong anthropogenic influence in and above the boundary layer of the NNW region may be from the uplift of emissions from the central region as the air masses passed over it on route to the western Pacific. Since the DC-8 did not sample over the Asian continent, there is really no way to separate these potential confounding influences
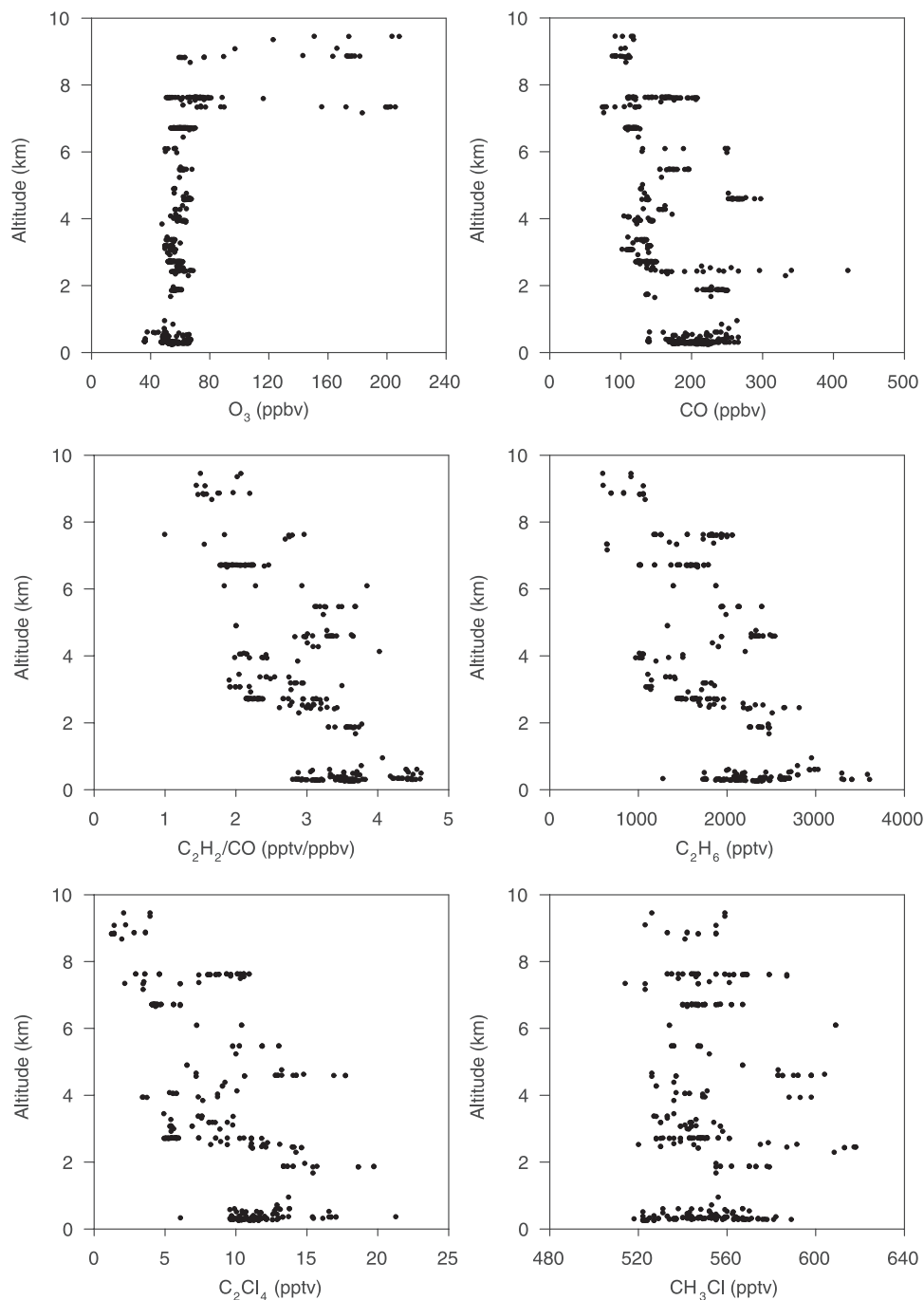
Figure 7. Vertical distributions of selected species in air masses originating in the North-Northwest source region.

from the two source regions. However, these two regions are kept separate because the NNW region trajectories originated at a much greater distance from the western Pacific. In addition, *Jordan et al.* [2003] demonstrated that the aerosol composition of the central region contained significantly more Ca^{+2} which separates it uniquely from the NNW region. Another possible explanation is transport of pollution from Europe or western Asia. However, only a small amount of the back trajectories in the NNW region originated over Europe [*Fuelberg et al.*, 2003]. This suggests that the long-range transport of European emissions was not significant

but nevertheless may have contributed to the air mass composition. Surface data has found evidence of a large CO plume from European fossil fuel combustion that is advected eastward over Siberia in the spring [*Rockmann et al.*, 1999]. Also, surface level data from the NOAA/CMDL sites in eastern Europe have found maximum CO mixing ratios to occur in the late winter/spring [e.g., *Novelli et al.*, 1998]. Previous work in the western Pacific has found evidence of a European pollution signal in Asian continental outflow. For example, the transport of European emissions to the western Pacific was a possible cause of high-altitude
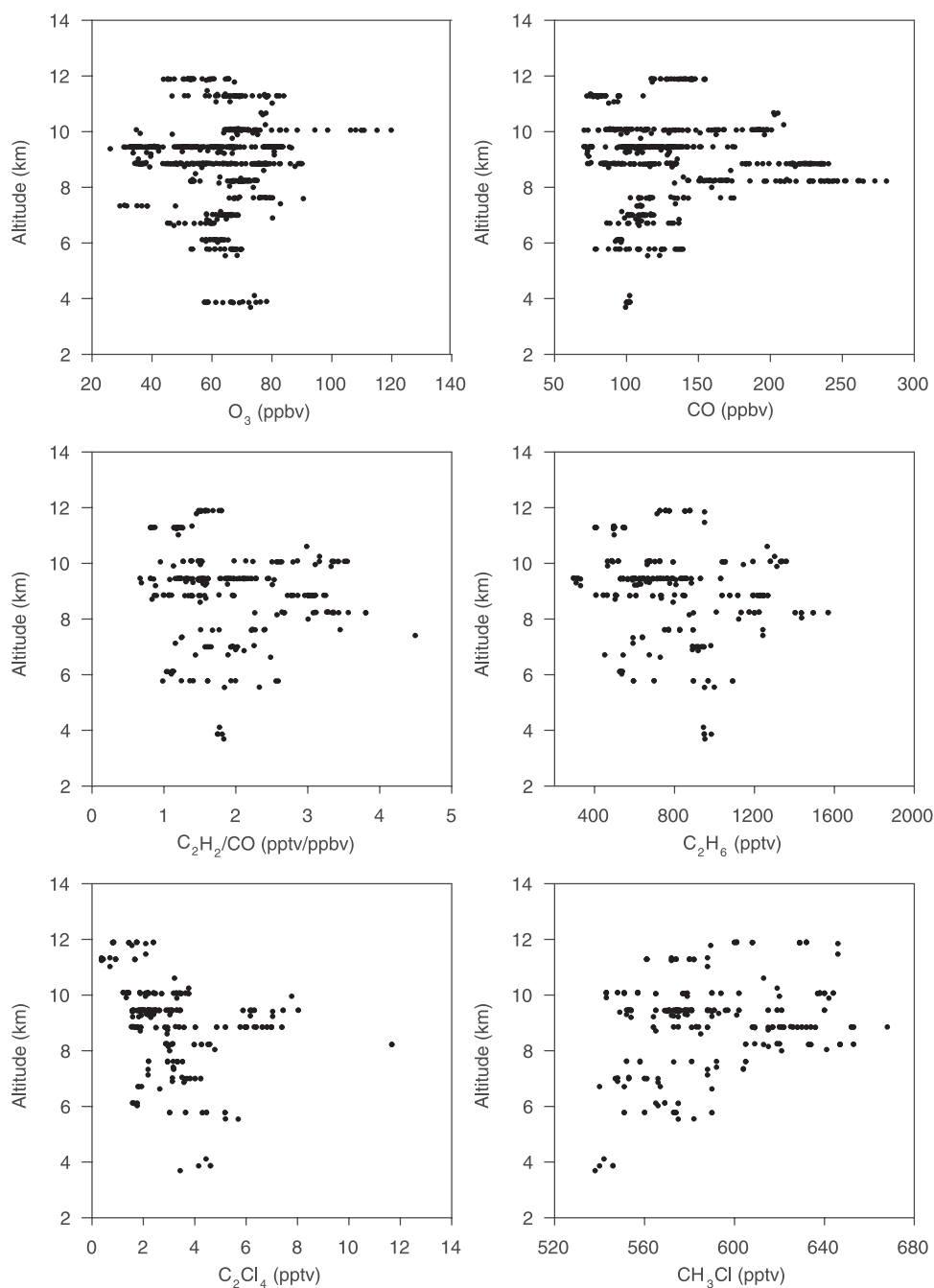
Figure 8. Vertical distributions of selected species in air masses originating in the West-Southwest source region.

species enhancements in the continental north group during PEM-West B [*Talbot et al.*, 1997]. In addition, anthropogenic emissions from Europe have been found to contribute significantly to Asian outflow at latitudes north of 40°N [*Bey et al.*, 2001]. However, any European influence south of 40°N indicated by 3-D simulations of CO mixing ratios was undetectable due to the strong Asian pollution signal [*Liu et al.*, 2003].

5.5. West-Southwest

[31]   The WSW region only exhibited continental outflow in the middle and upper altitudes. The vertical distributions

in the WSW and SE regions were similar in that significant outflow was present at high altitude (Figure 8, Table 5). Outflow from the WSW region occurred between 8 and 10 km. The CH_3OOH/H_2O_2 ratio was occasionally >1 in the outflow suggesting that some of the surface emissions may have been lifted by wet convection. Also, the lifting of emissions by midlatitude cyclones and their associated fronts appears to have been important for exporting emissions from the WSW region. This was the dominant transport pathway during TRACE-P [*Liu et al.*, 2003]. Furthermore, the C_2H_2/CO (>3) and C_3H_8/C_2H_6 (~0.2) ratios were enhanced above 7 km indicating that the outflow

contained relatively recent combustion inputs. As found in the SE region, background mixing ratios of several species, such as CO, O_3, C_2H_6, C_2H_2, C_3H_8, C_2Cl_4, and CH_3Cl, were also present intermittently in both the middle and upper troposphere indicating that substantial atmospheric processing had occurred. The similarities between the air mass composition in the WSW and SE regions may be a result of convective uplift of emissions from the SE region where they became entrained in the WSW region outflow.

[32] A striking feature of the WSW region is that both NO and CH_3Cl mixing ratios increased with altitude. The highest mixing ratios of NO were observed between 11 and 12 km, possibly from stratospheric inputs, lightning, or aircraft exhaust. Mixing ratios of O_3 (120 ppbv) and CO ($\sim$200 ppbv) were also enhanced around 10 km implying that these high-altitude air parcels contained a mixture of stratospheric and polluted air. *Talbot et al.* [2003] found that relationships between NO_x, O_3, and HNO_3 suggest a stratospheric source was responsible for enhanced NO_x in the upper troposphere. These results are consistent with data collected during the CARIBIC aircraft campaign that studied air masses at 10–11 km between Germany and the Indian Ocean [*Zahn et al.*, 2002]. This study area includes a portion of the WSW region. The CARIBIC study found that stratospheric inputs and photochemical production contributed equally to O_3 levels in the spring at middle latitudes. In contrast, photochemical production was responsible for the majority of the high-altitude O_3, with stratospheric inputs having a minimal influence, in the tropics [*Zahn et al.*, 2002]. This supports that both stratospheric and continental air was present in the upper troposphere of the WSW region and provides evidence that there are differences in the chemistry of the WSW and SE regions.

[33] NO and CH_3Cl were poorly correlated ($r^2 < 0.1$) above 7 km suggesting that biomass burning emissions were not responsible for the enhanced NO. *Liu et al.* [2003] concluded that CO emissions from African biomass burning were not detectable in air masses from the WSW region because any signal would be masked by the significant Asian pollution sources. Vertical lifting of emissions from the SE region is the most likely explanation for the enhanced CH_3Cl in the upper troposphere. However, an African contribution cannot be completely ruled out because a significant amount of the 5-day back trajectories in the WSW region originated over Africa. Also, biomass burning emissions from Africa have been shown to make a major contribution to Asian outflow at low latitudes and in the middle and upper troposphere [*Bey et al.*, 2001], and sources in the Middle East may have contributed to high-altitude outflow during PEM-West B [*Talbot et al.*, 1997].

[34] Recently injected anthropogenic emissions had a minimal influence on the composition of the middle troposphere in the WSW region. These air masses were aged several days and lacked strong correlations between key tracer species. C_2Cl_4 mixing ratios were enhanced $\sim$9 km ($\sim$12 pptv), however, it was poorly correlated with CO and C_2H_2 ($r^2 < 0.4$ at middle and high altitudes) which is indicative of aged industrial emissions. Similar to the SE region, the high altitude outflow contained combustion and biomass/biofuel burning emissions as indicated by correlations of CO, C_2H_2, and C_2H_6 with CH_3Cl ($r^2 \sim 0.62$–0.71). Furthermore, C_2H_2 and C_2H_6 were moderately correlated

with the biomass burning tracer, HCN ($r^2 = 0.78$ and 0.74, respectively). Among the high altitudes of the WSW, NNW, and SE regions, the highest mean and median mixing ratios of CO, C_2H_4, C_2H_2, C_6H_6, CH_3Cl, SO_2, PAN, and H_2O_2 were in air masses from the WSW region. Except for SO_2, these species are all characteristic of biomass burning. According to *Streets et al.* [2003], India is the second largest Asian source of SO_2, with power generation and industry being the largest sectors, and thus is a possible source of the enhanced SO_2. Similar results were found by the INDOEX campaign in 1999. Examination of air masses from India and SE Asia also found a minor contribution from industrial sources (low C_2Cl_4 and CH_3CCl_3) and an important influence in the free troposphere from biomass burning sources [*Scheeren et al.*, 2002].

6. Comparison With PEM-West B

[35] The TRACE-P and PEM-West B missions both occurred in late winter and spring but were conducted seven years apart. *Fuelberg et al.* [2003] concluded that the meteorological scenarios during the two missions were fairly similar; therefore meteorology most likely had a minimal influence on any variations in the tropospheric chemistry. Differences in the timing and design of the missions must also be considered. TRACE-P began later in February and lasted for a longer period of time than PEM-West B. As a result, the chemical composition may be influenced more by the characteristics of the springtime troposphere [*Fuelberg et al.*, 2003]. Furthermore, *Dibb et al.* [2003] suggest that the direct sampling of continental outflow, specifically near the Yellow Sea and the coast of China, during TRACE-P is a significant factor explaining different chemical and aerosol distributions between the two missions. This area was not probed during PEM-West B, and it clearly is a region heavily polluted by continental outflow.

[36] The three altitude ranges used in this paper are the same ranges used to characterize outflow during PEM-West B, thus allowing the vertical distributions to be compared. *Talbot et al.* [1997] separated the data at 20°N latitude into continental north and continental south groups. The NNW, central, coastal, and WSW regions are located at more northern latitudes and can thus be compared with the continental north group, and the SE and continental south regions can also be compared more or less directly. The median, maximum, and minimum mixing ratios of selected species are compared for the two missions in Tables 6–8. The "All" column represents all data from Flights 6–17 of TRACE-P, including data collected during spiral maneuvers. The WSW region is not included in the <2 km table (Table 6) because no boundary layer outflow was sampled. The central and coastal regions are not included in the >7 km table (Table 8) because they did not have high-altitude outflow due to their proximity to the flight paths.

6.1. Northern Regions

[37] The most striking difference between the two missions is that in all three altitude ranges the median O_3 mixing ratios were generally $\sim$10–20 ppbv higher during TRACE-P. Although the seasonal timing of the two missions was fairly similar, TRACE-P did extend two weeks

Table 6. Comparison of Mixing Ratios for Selected Species From the TRACE-P and PEM-West B Missions for Data <2 km[a]

		All	Central	Coastal	NNW	PEM West B-North	SE	PEM West B-South
O_3	Median	53	64	43	54	42	40	41
	Max	138	138	83	67	144	43	76
	Min	15	41	15	36	34	27	16
CO	Median	201	264	166	207	186	205	187
	Max	1113	1113	586	266	623	254	260
	Min	99	135	124	136	145	157	125
C_2H_2	Median	643	860	384	757	792	456	464
	Max	10403	10403	3264	1205	3356	627	835
	Min	122	308	125	268	463	369	176
C_2H_6	Median	2079	2540	1353	2353	2294	1155	1053
	Max	4888	4888	3598	3607	4323	1412	1528
	Min	661	1396	669	1276	1582	1105	655
SO_2	Median	348	2621	48	272	104	20	68
	Max	30736	30736	1554	2821	29770	45	2290
	Min	4	353	4	4	26	7	52
C_2Cl_4	Median	11	12	8	12	20	5	7.6
	Max	123	123	32	21	50	5	13
	Min	3	8	3	6	9	4	5.4

[a]The All column refers to all data from Flights 6–17. Units are in pptv except for O_3 and CO which are in ppbv.

Table 7. Comparison of Mixing Ratios for Selected Species From the TRACE-P and PEM-West B Missions for Data Between 2 and 7 km[a]

		All	Central	Coastal	NNW	WSW	PEM West B-North	SE	PEM West B-South
O_3	Median	59	61	60	60	65	45	57	56
	Max	206	76	69	206	91	69	72	66
	Min	19	47	43	48	29	23	27	16
CO	Median	122	135	132	126	108	138	88	88
	Max	530	219	272	420	175	300	331	203
	Min	70	104	107	74	78	72	74	81
C_2H_2	Median	252	313	255	304	190	471	93	65
	Max	2233	645	908	1098	602	1481	1210	847
	Min	46	209	181	117	81	28	48	50
C_2H_6	Median	1078	1334	929	1646	893	1614	528	555
	Max	3441	1968	1974	2813	1242	3771	1775	1601
	Min	401	1125	793	641	451	469	422	468
SO_2	Median	38	65	21	42	26	22	23	12
	Max	6989	284	120	6989	298	1432	415	26
	Min	5	10	10	7	10	5	6	12
C_2Cl_4	Median	4	6	5	7	3	13	2	5
	Max	115	10	11	18	6	27	16	8
	Min	1	4	3	2	2	3.4	1	4

[a]The All column refers to all data from Flights 6–17. Units are in pptv except for O_3 and CO which are in ppbv.

more into the springtime than PEM-West B which may result in increased O_3 production. Several companion papers found that this seasonal difference could be an important factor explaining the observed trace gas distributions during TRACE-P compared with PEM-West B [e.g., *Blake et al.*, 2003; D. D. Davis et al., Trends western North-Pacific ozone photochemistry as defined by observations from NASA's PEM-West B [1994] and TRACE-P [2001] field studies, submitted to *Journal of Geophysical Research*, 2003].

[38] Another noticeable difference between the two missions was the approximate factor of 2 lower mixing ratios of C_2Cl_4 during TRACE-P. This is likely a reflection of reduced emissions of industrial species, such as C_2Cl_4, CH_3CCl_3, and CCl_4, in Asia [*Blake et al.*, 2003]. CO mixing ratios were somewhat higher during TRACE-P at both low and high altitude. In the middle troposphere, CO mixing ratios were fairly similar particularly when comparing the heavily polluted central and coastal regions with the continental north group. At low and middle altitudes, C_2H_2 and C_2H_6 were generally lower during TRACE-P than they were during PEM-West B possibly because of increased OH oxidation in the spring or better emission controls in East Asia [*Streets et al.*, 2003]. The only exception is the central group in which C_2H_2 and C_2H_6 had higher median and maximum mixing ratios in the boundary layer due to the Shanghai plume. The median SO_2 mixing ratios were significantly larger in the low and middle altitudes of the "All," central, and NNW groups during TRACE-P. This result is unexpected given that *Streets et al.* [2003] estimated a 17.2% reduction in SO_2 emissions during 1994–2001 in East Asia. The fact that the higher median SO_2 mixing ratios were in the central and NNW regions may be evidence of the importance of the extensive sampling over the Yellow Sea during TRACE-P as explained by *Dibb et al.* [2003]. Also, China still dominates Asian sulfur emissions [*Streets et al.*, 2003] which may be a factor. Furthermore, ground based data

from the south China coast found similar results with higher O_3 and SO_2 during TRACE-P [*Wang et al.*, 2003].

6.2. Southern Regions

[39] A similarity between both missions is that mixing ratios for the six species used in this comparison were generally lower in the SE and continental south groups than in the northern TRACE-P regions and the continental north group. This is likely a result of the industrial cities and strong westerly outflow north of 20°N. In contrast to the northern groups, the median O_3 mixing ratios in the SE and continental south groups were remarkably similar in all altitude ranges. CO demonstrated the same trend as in the northern groups, with larger mixing ratios at low and high altitude during TRACE-P and with similar mixing ratios at middle altitudes.

Table 8. Comparison of Mixing Ratios for Selected Species From the TRACE-P and PEM-West B Missions for Data >7 km[a]

		All	NNW	WSW	PEM West B-North	SE	PEM West B-South
O_3	Median	53	151	66	51	32	35
	Max	208	208	120	119	70	69
	Min	18	59	26	25	18	21
CO	Median	102	105	121	94	88	81
	Max	341	118	281	316	223	111
	Min	63	88	70	62	67	57
C_2H_2	Median	146	164	208	131	89	67
	Max	1132	238	930	1513	609	274
	Min	47	138	47	35	47	16
C_2H_6	Median	631	916	731	672	514	543
	Max	1911	1076	1569	2463	1270	912
	Min	295	597	295	439	370	280
SO_2	Median	24	24	28	22	21	23
	Max	569	70	569	62	284	57
	Min	7	12	7	5	10	5
C_2Cl_4	Median	2	2	2	22	2	4.1
	Max	12	4	12	62	6	7.9
	Min	0	1	0	5	1	1.4

[a]The All column refers to all data from Flights 6–17. Units are in pptv except for O_3 and CO which are in ppbv.

Table 9. Comparison of Species Ratios for the Five TRACE-P Source Regions and the 2000 Asian Emissions Summary

Location	CO/CO_2	CO/CH_4	NO_x/SO_2	C_2H_6/C_3H_8
	Emissions Summary			
China	0.048	1.8	0.8	2.1
Other East Asia	0.014	2.2	2.7	1.3
Japan	0.009	3.7	3.8	1.1
Rep. of Korea	0.011	1.1	2.2	1.1
SE Asia	0.061	1.9	1.7	3.8
South Asia	0.054	1.1	1.1	2.7
India	0.053	1.1	1.2	2.6
	$\Delta CO/\Delta CO_2$	$\Delta CO/\Delta CH_4$	$\Delta NO_y/\Delta$ $(SO_2 + nss\ SO_4)$	$\Delta C_2H_6/\Delta C_3H_8$
	TRACE-P			
Central	0.022	1.6	0.3	2.6
Coastal	0.017	1.4	0.7	4.2
SE	0.013	3.4	4.8	5.2
NNW	1.017	1.4	0.5	2.8
WSW	0.020	2.1	3.6	5.2

In the middle troposphere, both the SE and continental south groups had a median CO value of 88 ppbv. C_2H_2, C_2H_6, and SO_2 did not exhibit any definite trends between the two missions. At low altitudes, C_2H_2 was fairly similar during the two missions while it appears higher in the SE group at middle and high altitudes. At low altitudes, SO_2 was significantly lower in the SE region compared to the continental south group. At high altitude in the WSW and SE regions, instances of significantly enhanced SO_2 were encountered as indicated by high maximum mixing ratios, but this did not occur in the upper troposphere during PEM-West B. C_2Cl_4 was also lower in the SE region than in the PEM-West B continental south group presumably reflecting reduced emissions of industrial species.

7. Comparison of Source Regions With Emissions Summary

[40] In order to gain insight on how well the 2000 Asian anthropogenic emissions summary developed by *Streets et al.* [2003] represented the Asian continent and how representatively the DC-8 sampled Asian outflow, emission ratios were compared with species ratios from each of the five source regions identified and characterized in this paper. The $\Delta CO/\Delta CO_2$, $\Delta CO/\Delta CH_4$, $\Delta C_2H_6/\Delta C_3H_8$, and $\Delta NO_y/\Delta(SO_2 + nss\text{-}SO_4)$ ratios for each of the five source regions were compared with the ratios from the emissions summary. The Δ refers to the difference between the measured and background mixing ratios and represents the impact from Asian emissions. The emissions summary provides data for NO_x and SO_2, so the NO_x/SO_2 ratio was compared with the observed $\Delta NO_y/\Delta(SO_2 + nss\text{-}SO_4)$ ratio. This latter ratio accounts for conversion of primary nitrogen and sulfur species present in the atmosphere after emission from various sources. Here $nss\text{-}SO_4$ represents non-sea-salt sulfate as presented by *Dibb et al.* [2003].

[41] The total anthropogenic emissions data was used from the emissions inventory. The median mixing ratios of all the data for each species in the five TRACE-P source regions were used in the calculations. Background mixing ratios were determined from Flight 5 as discussed previously in this paper. The background mixing ratios used were: CO = 70 ppbv, CO_2 = 370 ppmv, CH_4 = 1750 ppbv,

C_2H_6 = 420 pptv, C_3H_8 = 15 pptv, $SO_2 + nss\text{-}SO_4$ = 50 pptv, and NO_y = 60 pptv. These ratios only provide a rough comparison of the emissions summary and the TRACE-P data. The TRACE-P measurements were collected from several altitudes while the emission summary ratios may be more representative of surface measurements. TRACE-P ratios using only <2 km data were calculated and compared with the ratios using all the data from the three altitude ranges. There was very little difference between the ratios so we used the larger data set composed of the data from all three altitude bins. Also, the five source regions identified in this paper and the regions used in the emissions inventory are not exactly the same. Furthermore, the emission summary represents an entire year, but the TRACE-P source regions are only representative of 6 weeks of data. However, *Streets et al.* [2003] concluded that emissions during the TRACE-P period were near their average values.

[42] In general, there was remarkably good agreement and correspondence between the ratios for our five source regions and the emissions summary (Table 9). All calculated TRACE-P ratios were generally within the same order of magnitude as the emission summary ratios. The $\Delta CO/\Delta CO_2$ ratio for TRACE-P was ~0.02 in all five source regions which is within the estimated range of emission ratios, ~0.01–0.06. Both the CO/CH_4 and $\Delta CO/\Delta CH_4$ ratios were between 1 and 4, and both the C_2H_6/C_3H_8 and $\Delta C_2H_6/\Delta C_3H_8$ ratios were between ~1 and 5.2 for all regions compared. *Carmichael et al.* [2003b] examined numerous chemical species ratios using both observed and modeled results and found that high values of the C_2H_6/C_3H_8 ratio (~8) are representative of biomass burning in SE Asia while a lower ratio value (~2) reflects biofuel combustion. The $\Delta C_2H_6/\Delta C_3H_8$ values are highest in the SE and WSW source regions (~5.2), and the highest C_2H_6/C_3H_8 values from the emissions inventory are in the SE and South Asia groups, which is somewhat consistent with the *Carmichael et al.* [2003b] results. The $\Delta C_2H_6/\Delta C_3H_8$ ratio value in the central and NNW regions is ~2.7 which is near the expected value due to the higher use of fossil fuels and biofuels in central China.

[43] The $\Delta CO/\Delta CO_2$, $\Delta CO/\Delta CH_4$, $\Delta C_2H_6/\Delta C_3H_8$, and $\Delta NO_y/\Delta(SO_2 + nss\text{-}SO_4)$ ratios in the central and coastal regions were similar and comparable to the respective ratios

from the China region. For example, the NO_x/SO_2 ratio value of 0.77 for China is very comparable with the $\Delta NO_y/\Delta(SO_2 + nss\text{-}SO_4)$ ratios of 0.30 and 0.73 for the central and coastal regions, respectively. These ratio values are consistent with the observed NO_y/SO_x values (~ 0.2–0.5) for Chinese cities from *Carmichael et al.* [2003b]. The values are also fairly similar with the NO_x/SO_2 ratio (~ 0.31) based on emission estimates of *Kato and Akimoto* [1992]. The consistency of these four ratios suggests that the Asian emission inventory and DC-8 sampling during TRACE-P were fairly representative of Asian anthropogenic sources.

8. Conclusions

[44] In this paper we present the chemical composition of Asian outflow during the NASA TRACE-P mission in spring 2001. Outflow from the Asian continent had a significant influence on the tropospheric chemical composition over the western Pacific, and this impact extended into the central Pacific. The strongest outflow occurred between 20 and 40°N latitude and at low altitudes. Recent combustion emissions ($C_2H_2/CO \sim 4$) and enhanced species mixing ratios were encountered in the free troposphere and as far east as 150°E longitude reflecting rapid uplift and transport of continental emissions.

[45] Using 5-day backward trajectories, five source regions of continental outflow were identified. These regions were central, coastal, southeast, north-northwest, and west-southwest Asia. Outflow from all five regions was composed of a complex mixture of recent and photochemically aged combustion, industrial, and biomass/biofuel burning emissions. The outflow in each source region contained enhancements in many of the same anthropogenic species. A single pollution source did not dominate any of the air masses sampled from a specific source region. The distance of air mass origin from the western Pacific and the degree of processing in air masses influenced the vertical distribution and magnitude of the species enhancements. These results provide valuable documentation of species mixing ratios and the complexity of Asian continental outflow.

[46] The outflow in each source region contained CO that was at least 3 times larger than background (~ 70 ppbv) and relatively recent emissions as indicated by enhanced hydrocarbon ratios ($C_2H_2/CO \geq 3$ and $C_3H_8/C_2H_6 \geq 0.2$). As expected, the anthropogenic activity in East Asia had a direct impact on the chemical composition of air masses in the central and coastal regions. The highest mixing ratios for many species and most recent combustion emissions were found in the boundary layer of these two regions. CO, C_2H_2, CH_3Cl, and C_2Cl_4 were strongly correlated ($r^2 \sim 0.6$ to 0.98) in the central, coastal, and SE regions. Biomass burning was a large source of emissions in SE Asia; however, combustion and industrial sources were also significant. Recent combustion emissions were mixed with processed industrial and biomass/biofuel burning emissions in the NNW region. Aged industrial emissions were also found in the WSW region and were mixed with combustion and biomass burning emissions in the upper troposphere. Convection or lifting associated with mid-latitude cyclones was most likely responsible for the high altitude enhancements observed in the SE and WSW regions. Based on the backward trajectories, the long-range transport of emissions from Africa, the

Middle East, or Europe may have also made a minor contribution to the composition of air masses in the middle and upper troposphere of the NNW and WSW regions.

[47] A comparison between the TRACE-P and PEM-West B missions revealed some important differences. At northern latitudes, O_3 mixing ratios were higher during TRACE-P but were relatively unchanged in southern regions. At low and high altitude, CO was higher during TRACE-P, but it was quite similar in the middle troposphere. C_2H_2, C_2H_6, and SO_2 did not exhibit a definite trend between the two missions. C_2Cl_4 was lower at all altitudes during TRACE-P. The $\Delta CO/\Delta CO_2$, $\Delta CO/\Delta CH_4$, $\Delta C_2H_6/\Delta C_3H_8$, and $\Delta NO_y/\Delta(SO_2 + nss\text{-}SO_4)$ ratios for each source region were compared with the CO/CO_2, CO/CH_4, C_2H_6/C_3H_8, and NO_x/SO_2 ratios using data from the 2000 Asian emissions summary. The ratios agreed remarkably well indicating that the measurements obtained during TRACE-P and the emissions inventory were both representative of Asian emissions.

References

Bachmeier, M A. S., R. E. Newell, M. C. Shipham, Y. Zhu, D. R. Blake, and E. V. Browell, PEM-West A: Meteorological overview, *J. Geophys. Res.*, *101*, 1655–1677, 1996.

Berntsen, T. K., S. Karlsdottir, and D. A. Jaffe, Influence of Asian emission on the composition of air reaching the northwestern United States, *Geophys. Res. Lett.*, *26*, 2171–2174, 1999.

Bey, I., D. J. Jacob, J. A. Logan, and R. M. Yantosca, Asian chemical outflow to the Pacific in spring: Origins, pathways and budgets, *J. Geophys. Res.*, *106*, 23,097–23,113, 2001.

Blake, D. R., and F. S. Rowland, Urban leakage of liquefied petroleum gas and its impact on Mexico City air quality, *Science*, *269*, 953–956, 1995.

Blake, D. R., T.-Y. Chen, T. W. Smith Jr., J.-L. C.Wang, O. W. Wingenter, N. J. Blake, and F. S. Rowland, Three-dimensional distribution of non-methane hydrocarbons and halocarbons over the northwestern Pacific during the 1991 Pacific Exploratory Mission (PEM-West A), *J. Geophys. Res.*, *101*, 1763–1778, 1996.

Blake, N. J., D. R. Blake, T.-Y. Chen, J. E. Collins Jr., G. W. Sachse, B. E. Anderson, and F. S. Rowland, Distribution and seasonality of selected hydrocarbons and halocarbons over the western Pacific basin during PEM-West A and PEM-West B, *J. Geophys. Res.*, *102*, 28,315–28,331, 1997.

Blake, N. J., et al., NMHCs and halocarbons in Asian continental outflow during TRACE P: Comparison to PEM-West B, *J. Geophys. Res.*, *108*(D20), 8806, doi:10.1029/2002JD003367, in press, 2003.

Browell, E. V., et al., Large-scale ozone and aerosol distributions, air mass characteristics, and ozone fluxes over the western Pacific Ocean in late-winter/early-spring, *J. Geophys. Res.*, *108*(D20), 8805, doi:10.1029/2002JD003290, in press, 2003.

Carmichael, G. R., et al., Regional-scale chemical transport modeling in support of intensive field experiments: Overview and analysis of the TRACE-P observations, *J. Geophys. Res.*, *108*(D21), 8823, doi:10.1029/2002JD003117, in press, 2003a.

Carmichael, G. R., et al., Evaluating regional emission estimates using the TRACE-P observations, *J. Geophys. Res.*, *108*(D21), 8810, doi:10.1029/2002JD003116, in press, 2003b.

Crutzen, P. J., and M. O. Andreae, Biomass burning in the tropics: Impact on atmospheric chemistry and biogeochemical cycles, *Science*, *250*, 1669–1678, 1990.

Derwent, R. G., D. R. Middleton, R. A. Field, M. E. Goldstone, J. N. Lester, and R. Perry, Analysis and interpretation of air quality data from an urban roadside location in central London over the period from July 1991 to July 1992, *Atmos. Environ.*, *29*, 923–946, 1995.

Dibb, J. E., R. W. Talbot, E. Scheuer, G. Seid, M. Avery, and H. Singh, Aerosol chemical composition in Asian continental outflow during TRACE-P: Comparison to PEM-West B, *J. Geophys. Res.*, *108*(D21), 8815, doi:10.1029/2002JD003111, in press, 2003.

Duce, R. A., C. K. Unni, B. J. Ray, J. M. Prospero, and J. T. Merrill, Long-range atmospheric transport of soil dust from Asia to the tropical North Pacific: Temporal variability, *Science*, *209*, 1522–1524, 1980.

Fuelberg, H., C. M. Kiley, J. R. Hannan, D. J. Westberg, M. A. Avery, and R. E. Newell, Atmospheric transport during the Transport and Chemical Evolution over the Pacific (TRACE-P) experiment, *J. Geophys. Res.*, *108*(D20), 8782, doi:10.1029/2002JD003092, in press, 2003.

Gregory, G. L., J. T. Merrill, M. C. Shipham, D. R. Blake, G. W. Sachse, and H. B. Singh, Chemical characteristics of tropospheric air over the Pacific Ocean as measured during PEM-West B: Relationship to Asian outflow and trajectory history, *J. Geophys. Res.*, *102*, 28,275–28,285, 1997.

Heald, C. L., D. J. Jacob, P. I. Palmer, M. J. Evans, G. W. Sachse, H. Singh, and D. Blake, Biomass burning emission inventory with daily resolution: Application to aircraft observations of Asian outflow, *J. Geophys. Res.*, *108*(D21), 8811, doi:10.1029/2002JD003082, in press, 2003.

Heikes, B. G., Formaldehyde and hydroperoxides at Mauna Loa Observatory, *J. Geophys. Res.*, *97*, 18,001–18,013, 1992.

Heikes, B., M. Lee, D. Jacob, R. Talbot, J. Bradshaw, H. Singh, D. Blake, B. Anderson, H. Fuelberg, and A. M. Thompson, Ozone, hydroperoxides, oxides of nitrogen, and hydrocarbon budgets in the marine boundary layer over the South Atlantic, *J. Geophys. Res.*, *101*, 24,221–24,234, 1996.

Jacob, D. J., J. A. Logan, and P. P. Murti, Effect of Asian emissions on surface ozone in the United States, *Geophys. Res. Lett.*, *26*, 2175–2178, 1999.

Jacob, D. J., J. H. Crawford, M. M. Kleb, V. E. Connors, R. J. Bendura, J. L. Raper, G. W. Sachse, J. C. Gille, and L. Emmons, The Transport and Chemical Evolution over the Pacific (TRACE-P) mission: Design, execution, and overview of first results, *J. Geophys. Res.*, *108*(D20), 8781, doi:10.1029/2002JD003276, in press, 2003.

Jaffe, D. A., et al., Transport of Asian air pollution to North America, *Geophys. Res. Lett.*, *26*, 711–714, 1999.

Jordan, C. E., B. Anderson, R. W. Talbot, J. E. Dibb, H. E. Fuelberg, C. H. Hudgins, C. M. Kiley, R. Russo, E. Scheuer, G. Seid, K. L. Thornhill, and E. Winstead, Chemical and physical properties of bulk aerosols within four sectors observed during TRACE-P, *J. Geophys. Res.*, *108*(D21), 8813, doi:10.1029/2002JD003337, in press, 2003.

Kang, D., V. P. Aneja, R. G. Zika, C. Farmer, and J. D. Ray, Nonmethane hydrocarbons in the rural southeast United States national parks, *J. Geophys. Res.*, *106*, 3133–3155, 2001.

Kato, N., and H. Akimoto, Anthropogenic emissions of SO_2 and NO_x in Asia: Emission inventories, *Atmos. Environ.*, *26A*, 2997–3017, 1992.

Khalil, M. A. K., R. M. Moore, D. B. Harper, J. M. Lobert, D. J. Erickson, V. Koropalov, W. T. Sturges, and W. C. Keene, Natural emissions of chlorine-containing gases: Reactive Chlorine Emissions Inventory, *J. Geophys. Res.*, *104*, 8333–8346, 1999.

Li, Q., D. J. Jacob, R. M. Yantosca, C. L. Heald, H. Singh, M. Koike, Y. Zhao, G. W. Sachse, and D. G. Streets, A global 3-D model evaluation of the atmospheric budgets of HCN and CH_3CN: Constraints from aircraft measurements over the western Pacific, *J. Geophys. Res.*, *108*(D21), 8827, doi:10.1029/2002JD003075, in press, 2003.

Liu, H., D. J. Jacob, I. Bey, R. M. Yantosca, B. N. Duncan, and G. W. Sachse, Transport pathways for Asian combustion outflow over the Pacific: Interannual and seasonal variations, *J. Geophys. Res.*, *108*(D20), 8786, doi:10.1029/2002JD003102, in press, 2003.

Lobert, J. M., W. C. Keene, J. A. Logan, and R. Yevich, Global chlorine emissions from biomass burning: Reactive Chlorine Emissions Inventory, *J. Geophys. Res.*, *104*, 8373–8389, 1999.

McKeen, S. A., and S. C. Liu, Hydrocarbon ratios and photochemical history of air masses, *Geophys. Res. Lett.*, *20*, 2363–2366, 1993.

Merrill, J. T., M. Uematsu, and R. Black, Meteorological analysis of long range transport of mineral aerosols over the North Pacific, *J. Geophys. Res.*, *94*, 8584–8598, 1989.

Merrill, J. T., R. E. Newell, and A. S. Bachmeier, A meteorological overview for the Pacific Exploratory Mission-West Phase B, *J. Geophys. Res.*, *102*, 28,241–28,253, 1997.

Na, K., Y. P. Kim, and K. C. Moon, Diurnal characteristics of volatile organic compounds in the Seoul atmosphere, *Atmos. Environ.*, *37*, 733–742, 2003.

Novelli, P. C., K. A. Masarie, and P. M. Lang, Distributions and recent changes of carbon monoxide in the lower troposphere, *J. Geophys. Res.*, *103*, 19,015–19,033, 1998.

Rockmann, T., C. A. M. Brenninkmeijer, M. Hahn, and N. F. Elansky, CO mixing and isotope ratios across Russia: Trans-Siberian railroad expedition TROICA 3, April 1997, *Chemosphere Global Change Sci.*, *1*, 219–231, 1999.

Scheeren, H. A., J. Lelieveld, J. A. de Gouw, C. van der Veen, and H. Fischer, Methyl chloride and other chlorocarbons in polluted air during INDOEX, *J. Geophys. Res.*, *107*(D19), 8015, doi:10.1029/2001JD001121, 2002.

Simpson, I. J., N. J. Blake, E. Atlas, F. Flocke, J. H. Crawford, H. E. Fuelberg, C. M. Kiley, F. S. Rowland, and D. R. Blake, Photochemical production and evolution of selected C_2-C_5 alkyl nitrates in tropospheric air influenced by Asian outflow, *J. Geophys. Res.*, *108*(D20), 8808, doi:10.1029/2002JD002830, in press, 2003.

Singh, H. B., and P. B. Zimmerman, Atmospheric distribution and sources of nonmethane hydrocarbons, in *Gaseous Pollutants: Characterization and Cycling*, John Wiley, New York, 1992.

Singh, H. B., et al., In situ measurements of HCN and CH_3CN in the Pacific troposphere: Sources, sinks, and comparisons with spectroscopic observations, *J. Geophys. Res.*, *108*(D20), 8795, doi:10.1029/2002JD003006, in press, 2003.

Smyth, S., et al., Comparison of free tropospheric western Pacific air mass classification schemes for the PEM-West A experiment, *J. Geophys. Res.*, *101*, 1743–1762, 1996.

Streets, D. G., and S. T. Waldhoff, Biofuel use in Asia and acidifying emissions, *Energy*, *23*, 1029–1042, 1998.

Streets, D. G., and S. T. Waldhoff, Present and future emissions of air pollutants in China: SO_2, NO_x and CO, *Atmos. Environ.*, *34*, 363–374, 2000.

Streets, D. G., et al., An inventory of gaseous and primary aerosol emissions in Asia in the year 2000, *J. Geophys. Res.*, *108*(D21), 8809, doi:10.1029/2002JD003093, in press, 2003.

Talbot, R. W., et al., Chemical characteristics of continental outflow from Asia to the troposphere over the western Pacific Ocean during September–October 1991: Results from PEM-West A, *J. Geophys. Res.*, *101*, 1713–1725, 1996a.

Talbot, R. W., et al., Chemical characteristics of continental outflow over the tropical South Atlantic Ocean from Brazil and Africa., *J. Geophys. Res.*, *101*, 24,202–24,287, 1996b.

Talbot, R. W., et al., Chemical characteristics of continental outflow from Asia to the troposphere over the western Pacific Ocean during February–March 1994: Results from PEM-West B, *J. Geophys. Res.*, *102*, 28,255–28,274, 1997.

Talbot, R., J. Dibb, E. Scheuer, G. Seid, R. Russo, S. Sandholm, D. Tan, H. Singh, D. Blake, E. Atlas, G. Sachse, and M. Avery, Reactive nitrogen in Asian continental outflow over the western Pacific: Results from the NASA TRACE-P airborne mission, *J. Geophys. Res.*, *108*(D20), 8803, doi:10.1029/2002JD003129, in press, 2003.

Tang, Y., et al., The influences of biomass burning during TRACE-P experiment identified by the regional chemical transport model, *J. Geophys. Res.*, *108*(D21), 8824, doi:10.1029/2002JD003110, in press, 2003.

van Aardenne, J. A., G. R. Carmichael, H. Levy II, D. Streets, and L. Hordijk, Anthropogenic NO_x emissions in Asia in the period 1990–2020, *Atmos. Environ.*, *33*, 633–646, 1999.

Vay, S. A., et al., The influence of regional-scale anthropogenic emissions on CO_2 distributions over the western North Pacific, *J. Geophys. Res.*, *108*(D20), 8801, doi:10.1029/2002JD003094, in press, 2003.

Wang, C. J.-L., D. R. Blake, and F. S. Rowland, Seasonal variations in the atmospheric distribution of a reactive chlorine compound, tetrachloroethene ($CCl_2 = CCl_2$), *Geophys. Res. Lett.*, *22*, 1097–1100, 1995.

Wang, T., A. J. Ding, D. R. Blake, W. Zahorowski, C. N. Poon, and Y. S. Li, Chemical characterization of the boundary layer outflow of air pollution to Hong Kong during February–April 2001, *J. Geophys. Res.*, 2003.

Yienger, J. J., M. Galanter, T. A. Holloway, M. J. Phadnis, S. K. Guttikunda, G. R. Carmichael, W. J. Moxim, and H. Levy II, The episodic nature of air pollution transport from Asia to North America, *J. Geophys. Res.*, *105*, 26,931–26,945, 2000.

Zahn, A., C. A. M. Brenninkmeijer, W. A. H. Asman, P. J. Crutzen, G. Heinrich, H. Fischer, J. W. M. Cuijpers, and P. F. J. van Velthoven, Budgets of O_3 and CO in the upper troposphere: CARIBIC passenger aircraft results 1997–2001, *J. Geophys. Res.*, *107*(D17), 4337, doi:10.1029/2001JD001529, 2002.

————————————

E. Atlas and A. Fried, National Center for Atmospheric Research, Boulder, CO 80307, USA. (atlas@ucar.edu; fried@ucar.edu)

M. A. Avery, C. E. Jordan, G. W. Sachse, and S. A. Vay, NASA Langley Research Center, Hampton, VA 23665, USA. (m.a.avery@larc.nasa.gov; c.e.jordan@larc.nasa.gov; g.w.sachse@larc.nasa.gov; s.a.vay@larc.nasa.gov)

D. R. Blake and N. J. Blake, University of California, Irvine, Irvine, CA 92716, USA. (drblake@uci.edu; nblake@uci.edu)

J. E. Dibb, R. S. Russo, E. Scheuer, G. Seid, and R. W. Talbot, University of New Hampshire, Durham, NH 03820, USA. (jack.dibb@unh.edu; rrusso@resolution.sr.unh.edu; eric.scheuer@unh.edu; garry.seid@unh.edu; robert.talbot@unh.edu)

H. E. Fuelberg, Florida State University, Tallahassee, FL 32306, USA. (fuelberg@met.fsu.edu)

B. G. Heikes and J. Snow, University of Rhode Island, Narragansett, RI 02882, USA. (zagar@notos.gso.uri.edu; snow@gso.uri.edu)

S. T. Sandholm and D. Tan, Georgia Institute of Technology, Atlanta, GA 30332, USA. (scott.sandholm@eas.gatech.edu; tan@easlidar.gtri.gatech.edu)

H. B. Singh, NASA Ames Research Center, Moffett Field, CA 94035, USA. (hsingh@mail.arc.nasa.gov)